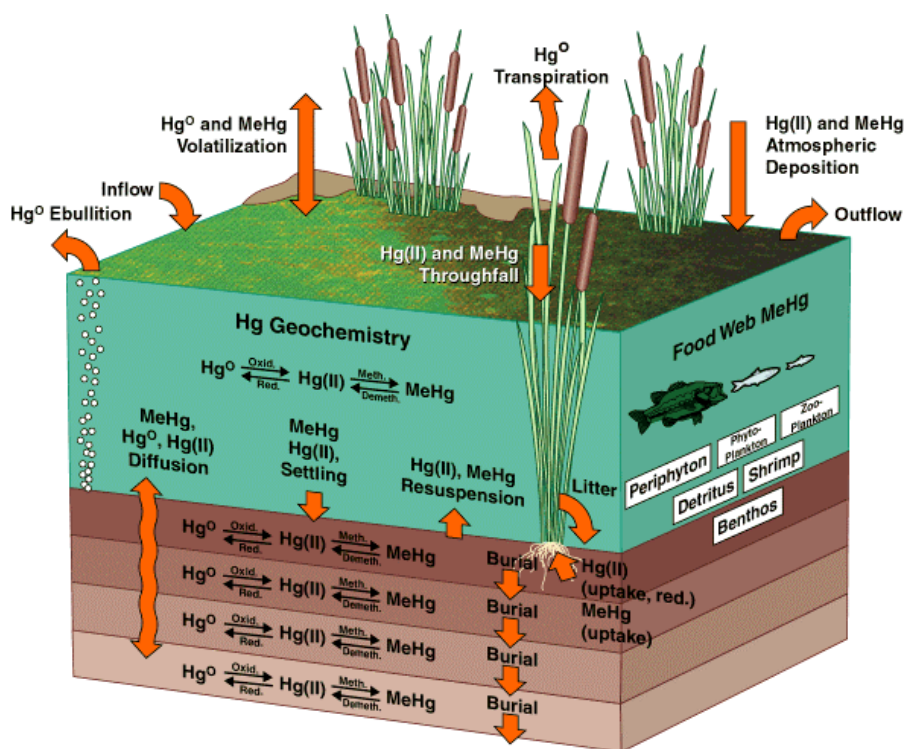


Appendix 7-3: Status of the Everglades Mercury Cycling Model

Tetra Tech, Inc. of Lafayette, California is the developer of the Mercury Cycling Model. Tetra Tech has been working under contract for DEP and SFWMD to adapt this model to the Everglades. As discussed in Chapter 7, DEP has recently undertaken a pilot project to determine the technical feasibility and information requirements for defining a Total Maximum Daily Load (TMDL) for atmospheric mercury for the Everglades. The Everglades Mercury Cycling Model (E-MCM) is fundamental to any attempt to control mercury in the Everglades. For the TMDL pilot project, Tetra Tech prepared the report on the E-MCM which follows.

Florida Pilot Mercury Total Maximum Daily Load (TMDL) Study: Application of the Everglades Mercury Cycling Model (E-MCM) to Site WCA 3A-15



Prepared for the United States Environmental Protection Agency and
Florida Department of Environmental Protection

Submitted by Reed Harris, Curtis D. Pollman, David Hutchinson and Don Beals
Tetra Tech Inc.
Lafayette, CA
March 2000

TABLE OF CONTENTS

SUMMARY	
1. INTRODUCTION	7
1.1 BACKGROUND ON THE FLORIDA PILOT MERCURY TMDL	7
2. AQUATIC MODELING OBJECTIVES.....	7
3. OVERVIEW OF THE EVERGLADES MERCURY CYCLING MODEL (E-MCM) 8	8
3.1 MERCURY FORMS	9
3.2 MODEL COMPARTMENTS	9
3.3 E-MCM PROCESSES	11
4. AQUATIC MODELING APPROACH.....	11
4.1 APPROACH TO MODEL CALIBRATION:	12
4.2 APPROACH TO DEVELOPING AN Hg(II) DOSE - FISH RESPONSE CURVE	12
4.3 APPROACH TO PREDICTING THE TIMING OF THE SYSTEM RESPONSE	13
4.4 APPROACH TO SENSITIVITY ANALYSIS	13
4.5 APPROACH TO YEAR-TO-YEAR VARIATIONS OF ATMOSPHERIC DEPOSITION	13
4.6 APPROACH TO CALCULATING UNCERTAINTY IN CURRENT ESTIMATES OF Hg DEPOSITION.....	14
5. SCENARIO DEVELOPMENT.....	17
5.1 WATER CONSERVATION AREA 3A -15	17
5.2 MODEL INPUTS FOR LONG-TERM AVERAGE CONDITIONS	18
5.2.1 <i>Cell Configuration:</i>	20
5.2.2 <i>Water Temperature and Incident Light</i>	20
5.2.3 <i>Hydrology</i>	22
5.2.4 <i>External Mercury Loadings</i>	24
5.2.5 <i>Water Chemistry Inputs</i>	25
5.2.6 <i>Food Web Inputs</i>	25
5.2.7 <i>Particle Dynamics</i>	28
6. RESULTS	30
6.1 MODEL CALIBRATION TO CURRENT LOADINGS	30
6.2 LONG-TERM Hg(II) DEPOSITION – FISH Hg RESPONSE CURVE.....	35
6.3 TIMING OF THE SYSTEM RESPONSE	37
6.4 SENSITIVITY ANALYSIS	39
6.5 YEAR-TO-YEAR VARIABILITY IN ATMOSPHERIC Hg(II) DEPOSITION	41
6.6 UNCERTAINTY REGARDING THE TRUE CURRENT RATE OF ATMOSPHERIC Hg(II) DEPOSITION.....	44
7. DISCUSSION.....	45
7.1 PREDICTED MERCURY CONCENTRATIONS	45
7.2 HOW FAST DOES THE WCA 3A-15 MARSH RESPOND TO CHANGES IN ATMOSPHERIC Hg(II) DEPOSITION?.....	46
7.3 PROCESSES CONTROLLING Hg CONCENTRATIONS AND DYNAMICS AT WCA 3A-15	47
7.4 EFFECTS OF ATMOSPHERIC Hg DEPOSITION ON FISH MERCURY CONCENTRATIONS.....	48
8. CONCLUSIONS	50
9. REFERENCES.....	51

LIST OF FIGURES

FIGURE 1. MERCURY CYCLING IN E-MCM	9
FIGURE 2. LOCATION OF WCA 3A-15.	17
FIGURE 3. ESTIMATED MEAN MONTHLY WATER TEMPERATURES FOR WCA 3A-15. ESTIMATED FROM HYDROQUAL (1997).....	21
FIGURE 4. MEAN MONTHLY INCIDENT LIGHT FOR WCA 3A-15. SOURCE: ESTIMATED FROM HYDROQUAL (1997).	21
FIGURE 5. ESTIMATED MEAN MONTHLY PRECIPITATION FOR WCA 3A-15. DATA FROM EVERGLADES FAMS SITES, 1992-1996. SOURCE: GILL <i>ET AL.</i> , (1999).	22
FIGURE 6. ESTIMATED MEAN MONTHLY SURFACE INFLOWS AND OUTFLOWS FOR WCA 3A-15. SOURCE:	23
FIGURE 7. ESTIMATED DAILY SURFACE WATER DEPTHS FOR WCA 3A-15 (SOURCE: 1996-97 ACME UNPUBLISHED DATA)	23
FIGURE 8. MONTHLY WET Hg(II) DEPOSITION RATES USED IN LONG-TERM E-MCM CALIBRATION. SOURCE: 1995-1996 DATA FROM KEELER <i>ET AL.</i> , 2000)	24
FIGURE 9. MONTHLY DRY/RGM Hg(II) DEPOSITION RATES USED IN LONG-TERM E-MCM CALIBRATION. SOURCE: 1995-1996 DATA FROM KEELER <i>ET AL.</i> , 2000)	24
FIGURE 10. FOOD WEB COMPARTMENTS IN E-MCM.....	25
FIGURE 11. FRACTIONS OF LARGEMOUTH BASS DIET (BY WEIGHT) REPRESENTED BY <i>GAMBUSIA</i> AND SUNFISH IN FINAL CALIBRATION.	26
FIGURE 12. OBSERVED AND CALIBRATED GROWTH RATES FOR LARGEMOUTH BASS.....	27
FIGURE 13. LENGTH VERSUS WEIGHT RELATIONSHIP FOR LARGEMOUTH BASS AT WCA 3A-15.	28
FIGURE 14. CALIBRATED PARTICLE FLUXES FOR SURFICIAL SEDIMENTS.....	29
FIGURE 15. PREDICTED LONG-TERM CONCENTRATIONS OF TOTAL MERCURY IN WCA 3A-15 SURFACE WATERS FOR CALIBRATION WITH CURRENT ATMOSPHERIC Hg(II) DEPOSITION = 30.94 $\mu\text{G}/\text{M}^2/\text{YR}$. OBSERVATIONS: KRABbenhofT <i>ET AL.</i> , (UNPUBLISHED DATA).....	31
FIGURE 16. PREDICTED LONG-TERM METHYLMERCURY CONCENTRATIONS IN WCA 3A-15 SURFACE WATERS FOR CALIBRATION WITH CURRENT ATMOSPHERIC Hg(II) DEPOSITION = 30.94 $\mu\text{G}/\text{M}^2/\text{YR}$. OBSERVATIONS: KRABbenhofT <i>ET AL.</i> , (UNPUBLISHED DATA).....	31
FIGURE 17. PREDICTED LONG-TERM HGT CONCENTRATIONS IN WCA 3A-15 SURFACE SEDIMENTS FOR CALIBRATION WITH CURRENT ATMOSPHERIC Hg(II) DEPOSITION = 30.94 $\mu\text{G}/\text{M}^2/\text{YR}$. OBSERVATIONS: GILMOUR <i>ET AL.</i> , 1998B	32
FIGURE 18. PREDICTED LONG-TERM MeHg CONCENTRATIONS IN WCA 3A-15 SURFACE SEDIMENTS FOR CALIBRATION WITH CURRENT ATMOSPHERIC Hg(II) DEPOSITION = 30.94 $\mu\text{G}/\text{M}^2/\text{YR}$. OBSERVATIONS: GILMOUR <i>ET AL.</i> , 1998B	32
FIGURE 19. PREDICTED LONG-TERM METHYLMERCURY CONCENTRATIONS IN SUNFISH IN WCA 3A-15 FOR CALIBRATION WITH CURRENT ATMOSPHERIC Hg(II) DEPOSITION = 30.94 $\mu\text{G}/\text{M}^2/\text{YR}$. OBSERVATIONS: LANGE <i>ET AL.</i> , UNPUBLISHED DATA	33
FIGURE 20. PREDICTED LONG-TERM METHYLMERCURY CONCENTRATIONS IN LARGEMOUTH BASS IN WCA 3A-15 FOR CALIBRATION WITH CURRENT ATMOSPHERIC Hg(II) DEPOSITION = 30.94 $\mu\text{G}/\text{M}^2/\text{YR}$. OBSERVATIONS: LANGE <i>ET AL.</i> , UNPUBLISHED DATA	33
FIGURE 21. PREDICTED LONG-TERM ANNUAL Hg(II) FLUXES IN $\mu\text{G M}^{-2} \text{YR}^{-1}$ FOR CALIBRATION TO ANNUAL ATMOSPHERIC Hg(II) DEPOSITION RATE OF 30.94 $\mu\text{G M}^{-2} \text{YR}^{-1}$	34
FIGURE 22. PREDICTED LONG-TERM ANNUAL MeHg FLUXES $\mu\text{G M}^{-2} \text{YR}^{-1}$ FOR CALIBRATION TO ANNUAL ATMOSPHERIC Hg(II) DEPOSITION RATE OF 30.94 $\mu\text{G M}^{-2} \text{YR}^{-1}$	35
FIGURE 23. PREDICTED Hg CONCENTRATIONS IN AGE 3 LARGEMOUTH BASS AS A FUNCTION OF DIFFERENT LONG-TERM CONSTANT ANNUAL RATES OF WET AND DRY Hg(II) DEPOSITION. PREDICTIONS ARE BASED ON CALIBRATION TO CURRENT LOADING OF 30.94 $\mu\text{G M}^{-1} \text{YR}^{-1}$	36

FIGURE 24. PREDICTED FRACTION OF CURRENT Hg CONCENTRATION IN AGE 3 LARGEMOUTH BASS AS A FUNCTION OF LONG-TERM REDUCTIONS IN Hg(II) DEPOSITION (WET AND DRY). PREDICTIONS ARE BASED ON CALIBRATION TO CURRENT LOADING OF $30.94 \mu\text{g m}^{-1} \text{yr}^{-1}$	37
FIGURE 25. PREDICTED DYNAMIC RESPONSE OF Hg CONCENTRATIONS IN LARGEMOUTH BASS IN WCA 3A-15 FOLLOWING DIFFERENT REDUCTIONS IN Hg(II) DEPOSITION. PREDICTIONS ARE BASED ON CALIBRATION TO CURRENT LOADING OF $30.94 \mu\text{g m}^{-1} \text{yr}^{-1}$	38
FIGURE 26. COMPARISON OF THE RATE AT WHICH AGE 3 LARGEMOUTH BASS CONCENTRATIONS APPROACH STEADY STATE FOLLOWING DIFFERENT REDUCTIONS IN Hg(II) DEPOSITION (SIMULATIONS ALL BASED ON CALIBRATION WITH CURRENT Hg(II) DEPOSITION = $30.94 \mu\text{g m}^{-2} \text{yr}^{-1}$).....	39
FIGURE 27. PREDICTED SENSITIVITY OF AGE 3 LARGEMOUTH BASS MERCURY CONCENTRATIONS IN WCA 3A-15 TO CHANGES IN VARIOUS INPUT VALUES. RESULTS ARE BASED ON CALIBRATION WITH CURRENT ATMOSPHERIC Hg(II) DEPOSITION = $30.94 \mu\text{g/m}^2/\text{yr}$	40
FIGURE 28. DISTRIBUTION OF ANNUAL ATMOSPHERIC DEPOSITION RATES USED FOR 500 YEAR SIMULATION. DISTRIBUTION SYNTHESIZED FROM FAMS DATA AS DESCRIBED IN SECTION 4.5.	41
FIGURE 29. INPUT ANNUAL ATMOSPHERIC Hg(II) DEPOSITION RATES AND PREDICTED Hg CONCENTRATIONS IN AGE 3 LARGEMOUTH BASS FOR 500 YEAR SIMULATION.....	42
FIGURE 30. DISTRIBUTION OF PREDICTED Hg CONCENTRATIONS IN AGE 4.75 LARGEMOUTH BASS FOR 500 YEAR SIMULATION. BIN SIZE = $0.02 \mu\text{g/g}$	43
FIGURE 31. PREDICTED DYNAMIC RESPONSE OF AGE 3 LMB CONCENTRATIONS TO A 50% REDUCTION IN ATMOSPHERIC Hg(II) DEPOSITION. RESULTS ARE SHOWN FOR THREE CALIBRATIONS. EACH CALIBRATION ASSUMES A DIFFERENT CURRENT RATE OF DEPOSITION.	44

LIST OF TABLES

TABLE 1. COMPARTMENTS AND MERCURY FORMS IN E-MCM.....	10
TABLE 2. STANDARD DEVIATION AND COEFFICIENT OF VARIATION OF “NORMALIZED” AVERAGE MONTHLY WET Hg DEPOSITION RATES IN SOUTH FLORIDA. DATA DERIVED FROM GILL <i>ET AL.</i> , (1999).....	14
TABLE 3. MODELED ANNUAL AND DRY DEPOSITION RATES DEVELOPED BY UMAQL AND THE ASSOCIATED ANNUAL UNCERTAINTIES (STANDARD DEVIATION). VALUES COMPUTED FROM MONTHLY ESTIMATES OF EACH FLUX COMPONENT AND ITS INHERENT UNCERTAINTY.	15
TABLE 4. SUMMARY OF PROPAGATED ERROR ANALYSIS OF EFFECTS OF MEASUREMENT ERROR (RAINFALL VOLUME AND Hg CONCENTRATION) ON ANNUAL RATES OF WET DEPOSITION... ..	15
TABLE 5. WATER CONSERVATION AREA 3A-15 CHARACTERISTICS	18
TABLE 6. SUMMARY OF DATA INPUTS BY MAJOR DATA TYPE CATEGORY.....	19
TABLE 7. DIETARY PATTERN OF LARGEMOUTH BASS USED FOR FINAL CALIBRATION.....	26
TABLE 8. DIETARY PATTERN OF SUNFISH USED FOR FINAL CALIBRATION.....	27
TABLE 9. DIETARY PATTERN OF <i>GAMBUSIA</i> USED FOR FINAL CALIBRATION.....	27
TABLE 10. VEGETATION-RELATED PARTICLE FLUXES IN THE WATER COLUMN: E-MCM INPUTS	29
TABLE 11. COMPARISON OF OBSERVED AND PREDICTED Hg CONCENTRATIONS IN SURFACE WATERS AND SEDIMENTS AT WCA 3A-15	30
TABLE 12. SUMMARY STATISTICS FOR PREDICTED Hg CONCENTRATIONS IN AGE 3 LARGEMOUTH BASS FOR 500 YEAR SIMULATION ($\mu\text{g g}^{-1}$ WET MUSCLE).....	43

Summary

The Clean Water Act Section 303(d) requires States to (1) identify and list waterbodies where State water quality standards are not being met and (2) establish “Total Maximum Daily Loads” (TMDLs) for those waters. A pilot project is currently underway to test methods relevant to the development of TMDLs for mercury from air sources. It combines field information with atmospheric and aquatic modeling of mercury transport and fate from source to receptor, in this case fish. The project is a cooperative, voluntary effort between the US EPA and the States of Wisconsin and Florida.

The pilot study is being conducted on a portion of the Florida Everglades within Water Conservation Area 3A (site 3A-15), 50 km west of Fort Lauderdale, and Devil’s Lake in Wisconsin (a small lake near Madison). Both of these waterbodies are on their States’ lists of “impaired” waterbodies, and have fish consumption advisories due to high levels of mercury in fish. The sites also were selected because of previous extensive mercury studies on-site.

This document describes the aquatic modeling undertaken with the Everglades Mercury Cycling Model (E-MCM) in support of the Florida pilot activities. E-MCM is a mechanistic simulation model that runs on Windows™-based computers. Using a mass balance approach, the model predicts time-dependent concentrations for three forms of mercury in water and sediments (dissolved and particulate phases), vegetation and a simplified food web that includes three fish populations.

The basic objective for aquatic modeling in the Florida pilot mercury TMDL study was to predict the magnitude and timing of the relationship between changes in atmospheric Hg(II) deposition and fish mercury concentrations in Everglades marsh area Water Conservation Area (WCA) 3A-15. Since this was a pilot exercise, an important component was to identify the strengths and weaknesses of the process. Since mercury concentrations in fish tend to increase with age and are higher in predatory fish towards the top of the food web, we selected age 3 largemouth bass as our standard.

Overall, our modeling approach was designed to allow us to predict the magnitude and timing of the response of fish mercury concentrations to changes in atmospheric Hg(II) deposition, while considering the model sensitivity to different inputs, uncertainty regarding true Hg(II) loading rates, and year to year variations in mercury deposition in the absence of a long-term record of mercury deposition at the site.

To calibrate the model, we used an estimate of $30.94 \mu\text{g m}^{-2} \text{yr}^{-1}$ for the mean annual atmospheric Hg(II) deposition (18.74 wet, 12.20 dry), based on Keeler *et al.*, (2000) who worked on the atmospheric modeling component of this study. Once the model was calibrated, simulations were run to predict the response of fish mercury concentrations to long-term sustained reductions in atmospheric Hg(II). We assumed that inflowing methylmercury and Hg(II) concentrations would also drop in proportion to the lower deposition rates. Simulations were run with Hg(II) deposition reductions of 25, 50, 75 and 85%. **A linear relationship is predicted, but the slope is not 1.0, i.e. there is not an exact 1:1 relationship predicted between percent changes in atmospheric Hg(II) deposition and percent changes in mercury concentrations in age 3 largemouth bass.** The deviation of the response curve from a slope of 1.0 reflects assumed methyl mercury deposition rates that are not affected by local source emissions, and long-term resupply from sediments. Thus, a load reduction of 75.6% is needed for predicted long-term average mercury concentrations in age 3 largemouth bass to drop from 1.64 to $0.5 \mu\text{g g}^{-1}$ wet muscle.

There is a lack of long-term mercury deposition data (e.g. 10 years or more) in the Everglades. To make initial estimates of the effects of year-to-year variations in Hg(II) deposition, we used the characteristics of monthly sampled data from 3 sites included in the Florida Atmospheric Mercury Study (FAMS) to synthesize a 500 year set of annual Hg(II) deposition rates. The results of this simulation predict the mercury concentration in age 3 largemouth bass exceeded $1.81 \mu\text{g g}^{-1}$ wet muscle 5% of the years. To reduce mercury concentrations of an age 3 largemouth bass from 1.81 to $0.5 \mu\text{g g}^{-1}$ wet muscle, E-MCM predicts a required decrease in atmospheric (Hg(II) deposition of 79%. It is also possible that, while reductions in Hg(II) loading to WCA 3A-15 may significantly reduce fish mercury concentrations, there may continue to be some fish over $0.5 \mu\text{g g}^{-1}$ wet muscle, even if all anthropogenic contributions to Hg(II) deposition are eliminated, unless additional remedial options are developed.

Regardless of the magnitude of the load reduction, fish mercury concentrations were predicted to change by 50% of the ultimate response within 6-7 years. Within 22 years, 90% of the ultimate predicted response has occurred. The actual magnitude of the change in fish Hg is of course still dependent on the magnitude of the load reduction. These predictions are not significantly altered because of uncertainty regarding true current Hg deposition rates and the effects of recalibration to different estimates of current deposition.

Predicted mercury concentrations in age 3 largemouth bass were most sensitive to factors associated with particle and vegetation fluxes, Hg(II) loading, methylation rates, and factors affecting fish diets and growth. While the dataset for model calibration for E-MCM at WCA 3A-15 was extensive in most regards, it would be useful to have improved mercury concentration data for the lower food web and vegetation. Furthermore, the lack of a long-term dataset for Hg(II) deposition required us to synthesize a dataset on the basis of limited data. There are also gaps in the state of knowledge of mercury cycling in the Everglades that resulted in modeling assumptions and impose uncertainty regarding the relationship between mercury deposition and fish mercury concentrations. These gaps should be addressed in future studies and include the location of and governing factors for methylation and demethylation, and mercury fluxes associated with vegetation and particles (litter, throughfall, transpiration, sedimentation, decomposition).

1. Introduction

1.1 Background on the Florida Pilot Mercury TMDL

The Clean Water Act Section 303(d) requires States to (1) identify and list waterbodies where State water quality standards are not being met and (2) establish “Total Maximum Daily Loads” (TMDLs) for those waters (US EPA 1999). TMDLs specify the amount of a pollutant that may be present in the water and still allow the waterbody to meet State water quality standards. Pollutant loads are allocated among point and non-point pollution sources, and include a margin of safety that accounts for uncertainty in the relationship between pollutant loads and characteristics of the waterbody. The allocations for water sources in TMDLs typically are implemented through existing Federal, State, Tribal, and local authorities. Year 2000 is the next year that States are required to develop their lists of impaired waterbodies, schedule for developing TMDLs, and submit them to the Environmental Protection Agency (EPA) for review and approval.

A pilot project is currently underway to test methods relevant to the development of TMDLs for mercury from air sources. It combines field information with atmospheric and aquatic modeling of mercury transport and fate from source to receptor, in this case fish. The project is a cooperative, voluntary effort between the US EPA and the States of Wisconsin and Florida. The pilot study is being conducted on a portion of the Florida Everglades known as Water Conservation Area 3A-15 (WCA 3A-15, 30 miles west of Fort Lauderdale), and Devil’s Lake in Wisconsin (a small lake near Madison). Both of these waterbodies are on their States’ lists of “impaired” waterbodies, and have fish consumption advisories due to high levels of mercury in fish.

Separate draft TMDL documents are being written for the studies in Wisconsin and Florida. Each draft TMDL will have supporting documents describing the atmospheric and aquatic modeling efforts. This document has been prepared in support of the Florida pilot mercury TMDL effort, and describes the associated aquatic modeling activities. The atmospheric deposition model used for the Everglades is called the Regional Meteorological Pollutant Chemistry and Transport Model, developed at the University of Michigan. Atmospheric modeling for the Everglades TMDL pilot work is described in a supporting document (Keeler *et al.*, 2000). The US EPA plans to issue a report on lessons learned from the pilot in 2000.

2. Aquatic Modeling Objectives

The overall objective of the aquatic modeling component of the pilot mercury TMDL for the Florida Everglades was:

To predict the magnitude and timing of the relationship between changes in atmospheric Hg(II) deposition and fish mercury concentrations in Everglades marsh area WCA 3A-15.

Specific sub-objectives included:

- Prediction of the reduction in Hg(II) loading to WCA 3A-15 necessary to maintain mercury concentrations in age 3 largemouth bass below 0.5 µg/g wet.

- ❑ Development of an Hg deposition – fish Hg response curve showing the effects of changing atmospheric Hg(II) deposition on long-term average mercury concentrations in largemouth bass in WCA 3A-15.
- ❑ Via sensitivity analysis, identification of the most important factors affecting fish mercury concentrations in WCA 3A-15..
- ❑ Quantification of the effects of uncertainty regarding actual Hg(II) deposition rates on model predictions.
- ❑ Estimation of the effects of year to year variability in Hg(II) deposition on fish mercury concentrations
- ❑ Identification of scientific gaps and needs in order to reduce uncertainty regarding the links between atmospheric Hg(II) deposition and fish mercury concentrations in Everglades marsh areas.

3. Overview of the Everglades Mercury Cycling Model (E-MCM)

A mercury cycling model has been developed to simulate the conditions found in marsh areas of the South Florida Everglades. The Everglades Mercury Cycling Model (E-MCM) (Tetra Tech 1999b) is an adaptation of the Dynamic Mercury Cycling Model for lakes (D-MCM) (Tetra Tech 1999a). E-MCM accommodates unique features of Everglades marshes from the perspective of mercury cycling in aquatic systems. Such features include shallow waters, a system of canals and managed water levels, a warm subtropical climate, high sun exposure, neutral to alkaline pH, high concentrations of dissolved organic carbon, large biomass of aquatic vegetation including periphyton, sawgrass, cattails and water lilies, and a wide range of nutrient levels and primary productivity. Field data (e.g. Gilmour *et al.*, 1998a, Gilmour *et al.*, 1998b, Krabbenhoft *et al.*, 1998) for parts of the Everglades have shown considerable spatial and temporal variability, with some locations apparently more conducive to methylmercury production and bioaccumulation.

E-MCM also incorporates recent advances made by researchers investigating mercury cycling in freshwater systems and in the Everglades specifically. These advances include an improved understanding of the factors governing methylation, demethylation, HgII reduction, food web mercury transfers, and the role of aquatic vegetation in the mercury cycle. Much of this work was done through the Aquatic Cycling of Mercury in the Everglades (ACME) project (e.g. Krabbenhoft *et al.*, 1998, Gilmour *et al.*, 1998a, Hurley *et al.*, 1998, Cleckner *et al.*, 1998).

E-MCM is a mechanistic simulation model that runs on Windows™-based computers. Using a mass balance approach, the model predicts time-dependent concentrations for three forms of mercury in water and sediments (dissolved and particulate phases), vegetation and a simplified food web (see Figure 1 and Table 1).

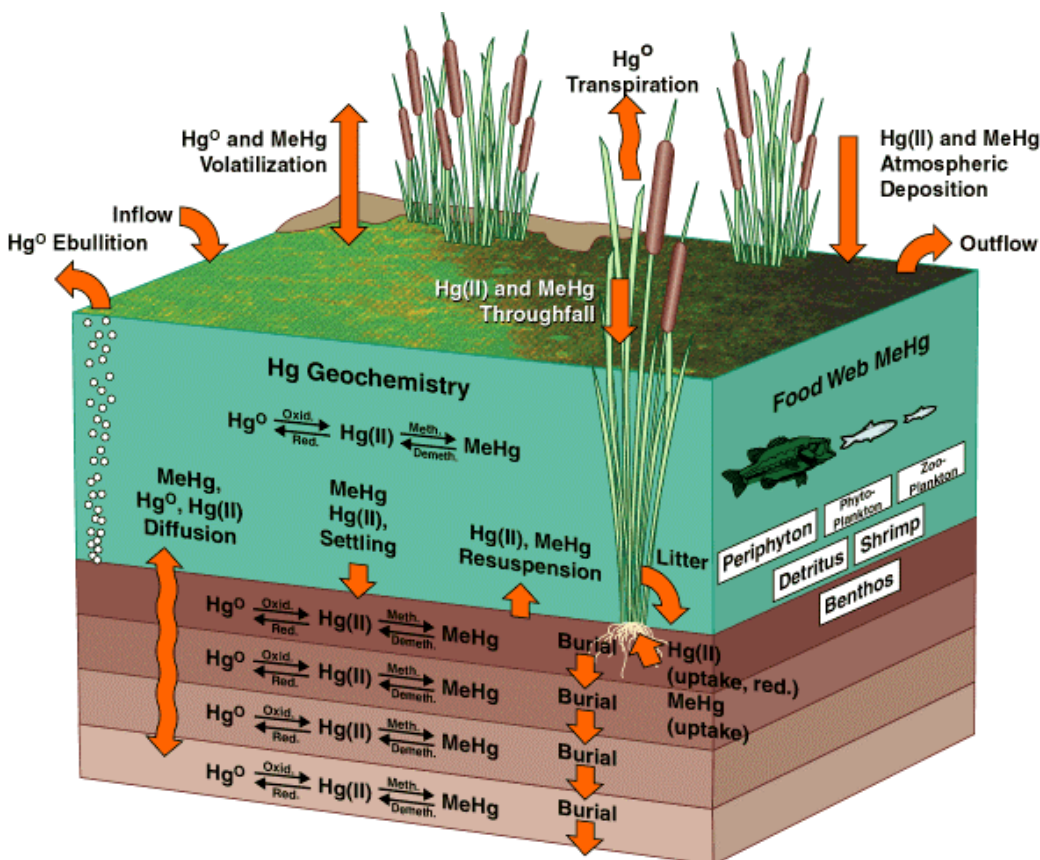


Figure 1. Mercury Cycling in E-MCM

3.1 Mercury Forms

There are three primary mercury forms in the E-MCM: methylmercury, Hg(II) and elemental mercury. Hg(II) is defined here as all mercury which is neither methylmercury nor elemental mercury. Provisions have also been made for some of the particulate Hg(II) on non-living solids to exchange slowly, while the remainder is assumed to exchange rapidly enough to assume instantaneous equilibrium partitioning.

3.2 Model Compartments

Model compartments include the water column, three macrophyte species (cattails, sawgrass, water lilies), four sediment layers and a food web (Table 1). The model has two types of particles in the water column: detritus and other suspended solids. For detrital, suspended, and sediment solids, provisions have been made for two types of Hg(II) exchange: (1) instantaneous and (2) slowly exchange governed by the kinetics of adsorption and desorption.

The water column in the Everglades is shallow, yet significant temperature gradients have been observed by ACME researchers (D. Krabbenhoft, unpublished data). The model therefore allows

for time-dependent thermal stratification and the formation of distinct surface and bottom water layer compartments if desired.

Mercury concentrations in the atmosphere are input as boundary conditions to calculate fluxes across the air/water interface (gaseous, wet deposition, dry particle deposition, deposition of reactive gaseous mercury).

Table 1. Compartments and Mercury Forms in E-MCM				
Compartment	Mercury Form			
	MeHg	Hg(II)	Elemental Hg	Solid HgS
Water Column (abiotic)				
Dissolved	•	•	•	
Non-living suspended particles*	•	•		•
Sediments				
Sediment Porewater	•	•	•	
Sediment Solids*	•	•		•
Vegetation				
Cattails	•	•		
Sawgrass	•	•		
Water lilies	•	•		
Food Web				
Detritus*	•	•		
Periphyton	•	•		
Phytoplankton	•	•		
Zooplankton	•	•		
Benthos	•	•		
Shrimp	•	•		
Non-Piscivore Fish Cohorts (up to 20)	•			
Omnivore Fish Cohorts (up to 20)	•			
Piscivore Fish Cohorts (up to 20)	•			

*Includes slowly and rapidly exchanging components for Hg(II).

The simplified food web consists of detritus, periphyton, phytoplankton, zooplankton, benthos, shrimp, *Gambusia*, bluegill/warmouth sunfish (grouped together), and largemouth bass. Fish mercury concentrations tend to increase with age, and are therefore followed in each year class (up to 20 cohorts) for each species). Bioenergetics equations developed for individual fish at the University of Wisconsin (Hewett and Johnson 1992) were modified to consider temperature dependent growth and coupled to methylmercury fluxes (Harris and Bodaly 1998). These fluxes for individual fish are then adapted to simulate year classes and entire populations (Tetra Tech 1999b)

3.3 E-MCM Processes

A detailed description of model processes and equations in E-MCM is provided in the user's guide (Tetra Tech 1999b). Major processes involved in the mercury cycle in an Everglades marsh are shown in Figure 1. These processes include surface inflows and outflows, vertical groundwater flow, instantaneous methylmercury partitioning between abiotic solids and dissolved complexes, instantaneous and slower adsorption/desorption kinetics for Hg(II) on abiotic solids, particulate settling, resuspension and burial, macrophyte related fluxes (throughfall, litter, root uptake, transpiration), atmospheric deposition, air/water gaseous exchange, in-situ transformations (methylation, demethylation, MeHg photodegradation, Hg(II) photoreduction), mercury kinetics in plankton, and methylmercury fluxes in fish populations (uptake via food and water, excretion, egestion, mortality, fishing).

4. Aquatic Modeling Approach

Overall, our aquatic modeling approach was designed to allow us to predict the magnitude and timing of the response of fish mercury concentrations to changes in atmospheric Hg(II) deposition, while considering the model sensitivity to different inputs, uncertainty regarding true Hg(II) loading rates, and year to year variations in mercury deposition in the absence of a long-term record of mercury deposition at the site.

Aquatic modeling for the Everglades pilot mercury TMDL included the following key components:

- ❑ *Selection of a site* known to have elevated fish mercury concentrations, as well as a high quality dataset: Water Conservation Area 3A-15
- ❑ *Data assembly*
- ❑ *Calibration* of E-MCM using estimates of long-term average annual conditions at site WCA 3A-15. The critical end point was mercury in largemouth bass, but the calibration examined total and mercury concentrations in each compartment for which data were available.
- ❑ *Development of a long-term steady-state dose-response curve* relating predicted long-term average fish mercury concentrations to different levels of long-term continuous atmospheric Hg(II) deposition. For example, if atmospheric deposition decreased to 50% of current levels and was maintained at the lower value, one question that immediately arises is at what levels would fish mercury concentrations ultimately stabilize? Model runs were carried out for several mercury deposition rates to develop the steady-state response curve.
- ❑ *Assessment of the predicted timing* of the response of fish mercury concentrations to different loadings of inorganic Hg(II).
- ❑ *Sensitivity analysis* of E-MCM predictions to various model input parameters, including atmospheric deposition rates of mercury.
- ❑ *Assessment of the effects of year-to-year variations* of atmospheric Hg(II) deposition.

- *Uncertainty analysis:* Quantifying the effects of uncertainty regarding true current atmospheric deposition rates on model predictions and study conclusions.

Further information on the approach to model calibration, sensitivity analysis, uncertainty analysis and assessment of year-to-year variations is provided below. Site selection is described in the overall draft TMDL document. Data assembly, model calibration and modeling results are presented in later sections of this document.

4.1 Approach to Model Calibration:

The model was initially calibrated on the basis of estimated long-term average conditions. Most of the data for the calibration were collected over a period of several years in the 1990's. Atmospheric mercury deposition data were collected over a 12 month period in 1995/96 (Keeler *et al.*, 2000), and the on-site mercury concentrations (except sportfish Hg) and fluxes were largely measured from 1995-99 during the ACME studies (e.g. Krabbenhoft *et al.*, 1998, Gilmour *et al.*, 1998a, Gilmour *et al.*, 1998b, Hurley *et al.*, 1998, Cleckner *et al.*, 1998). Mercury in largemouth bass, warmouth, and bluegill was measured by the Florida Department of Environmental Protection (T. Lange unpublished data).

For the purposes of this study we assumed that these datasets reasonably encompassed current mercury fluxes and concentrations at WCA 3A-15. We used the 1995/96 atmospheric Hg(II) deposition data and averaged site conditions from the 1995-98 data. We then ran simulations for 100 years with annual deposition patterns and site conditions repeating year over year, often with monthly frequencies for inputs. We examined the resulting mercury concentrations and fluxes once the system had effectively stabilized (i.e. concentrations were not changing year to year). These results were reported on a weekly basis for the 101st year of the simulation, so we could examine the seasonality of the predictions.

4.2 Approach to Developing an Hg(II) Dose - Fish Response Curve

One of the central questions for the pilot mercury TMDL exercise was to predict the relationship between atmospheric Hg(II) deposition and fish mercury concentrations. To make these predictions, we ran simulations with different Hg(II) loads maintained for a period of 200 years, long enough for fish mercury concentrations to effectively reach a steady state level for a given load. Simulations focused on the potential effects of Hg(II) load reductions on fish mercury concentrations, with predictions made 15, 25, 50, 75 and 100% of current estimates of total atmospheric Hg(II) deposition (wet and dry combined). These results were then combined in plots to show the shape of the Hg(II) dose – long-term fish Hg response curve. We chose age 3 largemouth bass as a benchmark standard for our analyses.

When running simulations with Hg(II) deposition rates other than current loadings, we had to make assumptions about the likely changes in atmospheric methylmercury deposition, and inflowing methylmercury and Hg(II) concentrations. We kept atmospheric methylmercury deposition rates constant for all simulations. We adjusted inflowing methylmercury and Hg(II) concentrations in proportion to the reduction in atmospheric Hg(II) deposition.

4.3 Approach to Predicting the Timing of the System Response

To examine the time required for fish mercury concentrations to respond to load reductions, we ran simulations for 200 years with Hg(II) deposition held constant at current levels until fish mercury concentrations were stable, then instantaneously reduced the load in a step function manner to a constant lower load. We examined fish Hg response dynamics for load reductions of 25, 50, 75 and 85% from current atmospheric deposition rates to develop the response curve.

4.4 Approach to Sensitivity Analysis

It is important to understand which inputs in the model have the greatest influence on predicted fish mercury concentrations. A standard approach is the use of a sensitivity analysis, varying selected input parameters a given amount, in this case plus or minus 50%. In some cases, a change to an input value of 50% did not make physical sense; for example one could not increase the fraction of the marsh covered by vegetation from 80 to 130 percent. In such cases, a lesser increase was tested. To allow a common basis to compare the effects of different inputs, results were plotted as the percent change in fish mercury concentration vs. percent change in the input variable ($\Delta Hg_{\text{fish}}\% / \Delta \text{Input}\%$).

It should be noted that this type of traditional sensitivity analysis does not account for the actual variability/uncertainty associated with each input. Some inputs may vary proportionately more than others. This can be accommodated via a Monte Carlo approach that uses probabilistic distributions for key inputs, but is beyond the scope of the current exercise. A Monte Carlo version of E-MCM is currently under development.

4.5 Approach to Year-to-Year Variations of Atmospheric Deposition

It is also important in a TMDL study to consider year-to-year variability in mercury deposition. No long-term dataset (e.g. 20 years or more) was available in terms of atmospheric deposition on-site. An approach was therefore used whereby we synthesized an artificial set of 500 mean annual Hg(II) deposition rates based on data from three of the FAMS sites in the region. These sites had comprehensive deposition data spanning 2-4 year periods. The 500 point synthesized dataset had lognormal distribution characteristics with the desired mean and standard deviation values.

Inherent in this approach were several key assumptions:

1. Deposition is constant over the long-term but varies annually about some mean value, and can be described statistically as a lognormal distribution.
2. Wet deposition rates measured at the Florida Atmospheric Mercury Study (FAMS) south Florida sites between 1993 and 1996 are adequate to describe the variance of this distribution.
3. The coefficient of variation for total deposition is similar to values measured for wet deposition rates.

Data for analysis were restricted to years (within each site) that had ≥ 9 months data. The FAMS marine background site Crawl Key was precluded from analysis because its rainfall and deposition patterns were clearly dissimilar from the interior Everglades sites. Three sites had sufficient year-to-year data to compute standard deviations: Everglades National Park (EG), Fakahatchee Strand (FS), and Tamiami Trail (TT) (Table 2). For each site, total wet deposition was summed for each year with greater than 8 months of data, and then divided by the number of

months within each year to yield a “normalized” monthly deposition rate for each year. Assuming that annual deposition is lognormally distributed, each normalized monthly deposition rate was then log-transformed, and the standard deviations (σ) and coefficients of variation (c.v.) across the years were computed for each site. This resulted in an average c.v. of 26.4% for the three sites.

The synthetic total deposition dataset was then constructed based on the estimated annual average total Hg deposition rate of $30.94 \mu\text{g}/\text{m}^2\text{-yr}$ developed by Keeler *et al.*, (2000). A normally distributed data set was first produced ($n = 500$) with a mean value of 1.0 and σ of 0.264. This data set was then exponentially transformed and scaled to produce a data set with an arithmetic mean value of 30.94.

Variations in largemouth bass concentrations were then computed by first running E-MCM with a fixed deposition rate of $30.94 \mu\text{g m}^{-2} \text{ yr}^{-1}$ for 200 years to achieve steady state conditions. Using the synthesized total deposition data set to simulate annual deposition variability, the model was then run an additional 500 years, with fish mercury concentrations recorded each year.

Table 2. Standard deviation and coefficient of variation of “normalized” average monthly wet Hg deposition rates in South Florida. Data derived from Gill *et al.*, (1999).

Site	N (years)	Ln-transformed Average Normalized Monthly Deposition	Standard Deviation	Coefficient of Variation
Everglades National Park	3	0.627	0.085	0.136
Fakahatchee Strand	4	0.672	0.209	0.311
Tamiami Trail	2	0.605	0.208	0.344

4.6 Approach to Calculating Uncertainty in Current Estimates of Hg Deposition

There is uncertainty inherent in our estimates of average annual wet and dry Hg(II) deposition arising from (but not limited to) analytical and field collection errors, errors induced from extrapolating from sites where Hg wet deposition has been measured to site 3A-15, and errors in modeling source-receptor relationships, including errors in emission estimates and errors in simulating meteorological conditions.

To accommodate uncertainty in the current Hg(II) deposition rates, we calibrated E-MCM for three loading scenarios:

- The current mean annual load: $30.94 \mu\text{g m}^{-2} \text{ yr}^{-1}$
- The upper and lower limits encompassing 95% of the likely estimates for current total deposition rates (discussed below): $= 36.74$ and $25.14 \mu\text{g m}^{-2} \text{ yr}^{-1}$ respectively

For each of the three loading rates, the model was calibrated to achieve the current observed total and methylmercury concentrations in the marsh, including fish. Thus the predicted fish mercury

concentrations were nearly identical in each calibration, but some rate constants were altered between scenarios. Once the model was calibrated for three different loading scenarios, we tested whether different calibrations significantly affected the study conclusions.

Table 3 summarizes the modeled annual wet and dry deposition rates developed by Keeler *et al.*, (2000) and the associated annual uncertainties, which are largely due to uncertainties in modeled meteorology.

Table 3. Modeled annual and dry deposition rates developed by UMAQL and the associated annual uncertainties (standard deviation). Values computed from monthly estimates of each flux component and its inherent uncertainty.

Flux Component	Deposition ($\mu\text{g m}^{-2} \text{ yr}^{-1}$)	σ ($\mu\text{g m}^{-2} \text{ yr}^{-1}$)
Wet Deposition	18.74	1.57
Dry Deposition (RGM & particles)	12.20	2.03
Total Deposition	30.94	2.57

There also is uncertainty in the FAMS deposition measurements used to calibrate the models used by Keeler *et al.* As part of FAMS, replicates (and occasional triplicate) samples were collected in the field monthly. These replicates provide a measure of the combined uncertainty in the both field collection and laboratory analysis. This error was generally quite low, with the coefficient of variation (CV) averaging only 6.57% for all sites ($n = 348$ data pairs). There also is error associated with rainfall measurements which, according to Winter (1981), is ca. 10%.

Assuming a constant rainfall measurement of 10%, the error in monthly deposition estimates and the propagated error in the derived annual deposition rates can be calculated. Table 4 summarizes the results of this analysis for the Everglades FAMS sites and FAMS sites proximal to the Everglades.

Table 4. Summary of propagated error analysis of effects of measurement error (rainfall volume and Hg concentration) on annual rates of wet deposition.

FAMS Site	CV (%)
AT	5.55
EG	4.10
EN	4.50
FS	4.97
TT	4.58
Overall Average	4.74

Note: Table shows the coefficient of variation obtained as an average across each study year for each site.

The errors from the two sets of analyses were combined by assuming that the modeled estimate can be given by:

$$J_{\text{estimated}} \pm \sigma_{\text{estimated}} = (M_{\text{measured}} \pm \sigma_{\text{measured}}) \cdot (J_{\text{modeled}} \pm \sigma_{\text{modeled}})$$

where J is the total deposition flux ($\mu\text{g}/\text{m}^2\text{-yr}$), σ is the standard deviation of the parameter estimate, and M is a term included to account for the effects of measurement uncertainty on the calibrated model. M is assumed equal to 1 with an error of 4.74%, while $J_{\text{modeled}} = 30.94$ with an error of 8.30%. The propagated CV is calculated as:

$$CV_{\text{estimated}}^2 = CV_{\text{measured}}^2 + CV_{\text{modeled}}^2$$

$\sigma_{\text{estimated}}$ thus equals 2.96 ($CV_{\text{estimated}} = 9.57\%$).

Upper and lower limits encompassing 95% of the likely estimates for current total deposition rates can then be computed:

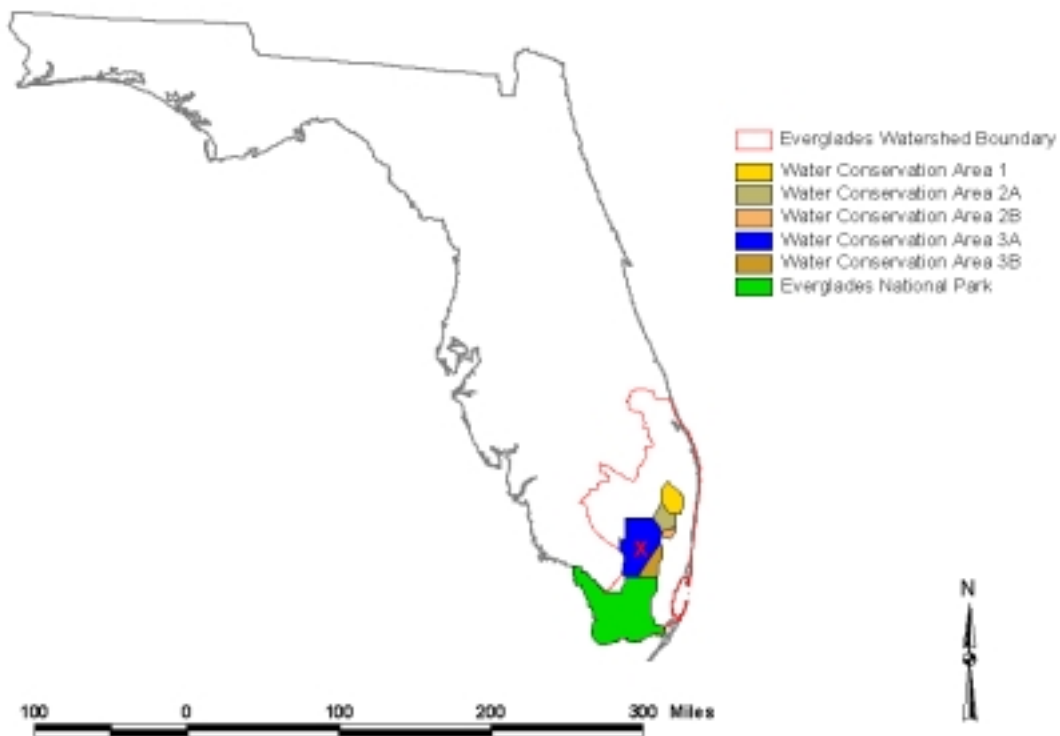
$$J_{\text{estimated}} \big|_{\text{upper bound}} = 30.94 + 2.96 \cdot 1.96 = 36.74$$

$$J_{\text{estimated}} \big|_{\text{lower bound}} = 30.94 - 2.96 \cdot 1.96 = 25.14$$

5. Scenario Development

5.1 Water Conservation Area 3A -15

Water Conservation Area 3A (WCA 3A) in the Everglades is located about 50 km west of Fort Lauderdale (US EPA 1999) and has an area of approximately 1,800 km² (Figure 2). Water Conservation Area 3A-15 was selected because it has elevated mercury concentrations in



largemouth bass, and has been extensively studied in terms of mercury cycling.

Figure 2. Location of WCA 3A-15.

Characteristics of WCA 3A-15 are summarized in Table 5.

Table 5. Water Conservation Area 3A-15 Characteristics	
Parameter	Value
Area modeled	1 km x 1 km
Surface water depth	0.2 to 0.7 m
Air Temperatures (monthly means)	12 to 30 C
Productivity	Low (oligotrophic)
Flow pattern	Surface flow
Stratification	Intermittent
Anoxia	Yes
Dissolved organic carbon	~ 16 mg L ⁻¹
Surface water pH	~ 7.2
Surface water chloride	~ 5 mg L ⁻¹
Surface water sulfate	100 µeq L ⁻¹
Sedimentation rate:	< 1 cm yr ⁻¹
TSS	~ 2 mg/L
Macrophytes	Includes sawgrass, cattails, water lilies
Fraction of marsh with open water	<50%
Periphyton density	dense
Top predator fish	Largemouth bass

5.2 Model Inputs for Long-term Average Conditions

In response to the mercury issue in the Everglades, several agencies initiated research and monitoring programs in the 1990's. These include the ACME studies (1995-present), FAMS (Guentzel *et al.*, 1995; Gill *et al.*, 1999), a USEPA Regional Environmental Monitoring and Assessment (REMAP) project in 1994-1995, with data on water, soil, vegetation and fish at 125 sites; a study by the Southwest Florida Water Management District which sampled 9 surface water control sites over three years (1993-1995); and a long-term Florida Game and Freshwater Fish database on mercury in largemouth bass and other fishes. As a result, there are extensive air, water, soils, and biota data on mercury at WCA 3A-15 (US EPA, 1999). Input data types and sources for WCA 3A-15 long-term simulations are summarized in Table 6.

Table 6. Summary of Data Inputs by Major Data Type Category	
Data Type	Parameter Estimate and Source
Hydrologic Data	
Precipitation	Monthly means from FAMS sites AT, FS, and TT, 1992-1996 (Gill <i>et al.</i> , 1999)
Surface water elevations	Direct daily measurements (USGS, Miami Florida Sub District Office)
Surface Flow	Monthly means computed based on cell size configuration, assumed hydraulic retention time, and precipitation seasonality.
Physical Data	
Temperature and incident light	Monthly means estimated from NOAA gauge data at West Palm Beach, 10/89 to 9/94 – Hydroqual (1997)
Soil moisture content	Assumed 100% saturation at all times
Mercury Loadings	
Wet Hg(II) deposition	Keeler <i>et al.</i> , (2000)
Dry Hg(II) deposition	Keeler <i>et al.</i> , (2000)
Leaf Area Index	3 (assumed)
Upstream Surface water concentrations – Hg(II)	Based on average for 2BS = 2.32 ng/L (n=9)
Upstream Surface water concentrations – MeHg (unfiltered)	Based on average for 2BS = 0.46 ng/L (n=9)
Surface Water Chemistry	
DOC	ACME data (n = 8) (G. Aiken, USGS unpublished data)
pH and DO	Limno-Tech (1996)
SO ₄ ²⁻	~100 µeq/L (Gilmour <i>et al.</i> , 1998b)
Hg Concentrations in Marsh	
Surface water Hg _{total} and MeHg (filtered and unfiltered)	1995-1998 data from ACME (D. Krabbenhoft, unpublished data)
Elemental Hg (DGM)	20 – 40 pg/L (Krabbenhoft <i>et al.</i> , 1998)
Sediment Hg	(Gilmour <i>et al.</i> , 1998b)
Sediment porewater chemistry	Gilmour <i>et al.</i> , 1998b)
Food Web and Vegetation	
Fish growth (LMB) and Hg concentrations	T. Lange (unpublished data)
<i>Gambusia</i> Hg concentrations	D. Krabbenhoft (unpublished data)
Fish diets	Cleckner and Gorski (ACME unpublished data)
Fish biomasses	Marshwide average = 40 kg/ha (wet) (Jordan, 1996 cited in Ambrose <i>et al.</i> , 1997)
Macrophyte and periphyton biomasses and	Ambrose <i>et al.</i> , (1997)

Table 6. Summary of Data Inputs by Major Data Type Category	
turnover rates	
Macrophyte Hg _{tot} concentrations	USGS collected samples, FDEP funded analyses by Frontier Geosciences
Shrimp and zooplankton MeHg concentrations	100 - 200 ng/g (dry) (Cleckner, personal communication)
Benthos MeHg and Hg _{tot} concentrations	No data
Periphyton MeHg and Hg _{tot} concentrations	(Cleckner <i>et al.</i> , 1998)
Particle Dynamics	
Hg(II) Sorption	Calibrated
Sediment accumulation rates	Derived from Delfino <i>et al.</i> , (1993 and 1994)
Sediment decomposition rates	Derived from litter turnover rates and net mass sedimentation.

Additional information describing inputs used in simulations is provided below:

5.2.1 Cell Configuration:

Unlike a lake, an Everglades marsh does not have defined boundaries. Dimensions for a marsh “cell” must therefore be selected. We chose a 1 km x 1 km cell size to represent an area of homogeneous conditions within WCA 3A-15; this size is consistent with the spatial resolution of other hydrologic and aquatic cycling models such as the Everglades Landscape Model (ELM) (Fitz *et al.*, 1996) currently under development or currently applied to the Everglades. This choice is somewhat arbitrary insofar as there are few data available to define the appropriate dimensions of a homogeneous cell in this system, particularly with respect to mercury dynamics. The choice of cell size also has significant implications for the relative importance of atmospheric, inflowing, and in-situ loadings of total and methylmercury to the cell. For a square cell shape, a smaller the cell area results in a greater importance of inflows relative to other sources. The effects of different inflow rates were tested during the sensitivity analysis and are discussed below.

Four sediment layers were included in the model, similar to Ambrose *et al.*, 1997. The layer thicknesses were 3, 5, 20, and 20 cm respectively, starting with the surficial layer.

5.2.2 Water Temperature and Incident Light

Water temperatures were assumed to be the same as air temperatures. Daily data for air temperature and incident light were available from NOAA data collected at West Palm Beach, from October 1989 to September 1994 Hydroqual (1997). From these data, mean monthly temperatures and incident light were estimated as shown in Figures 3 and 4.

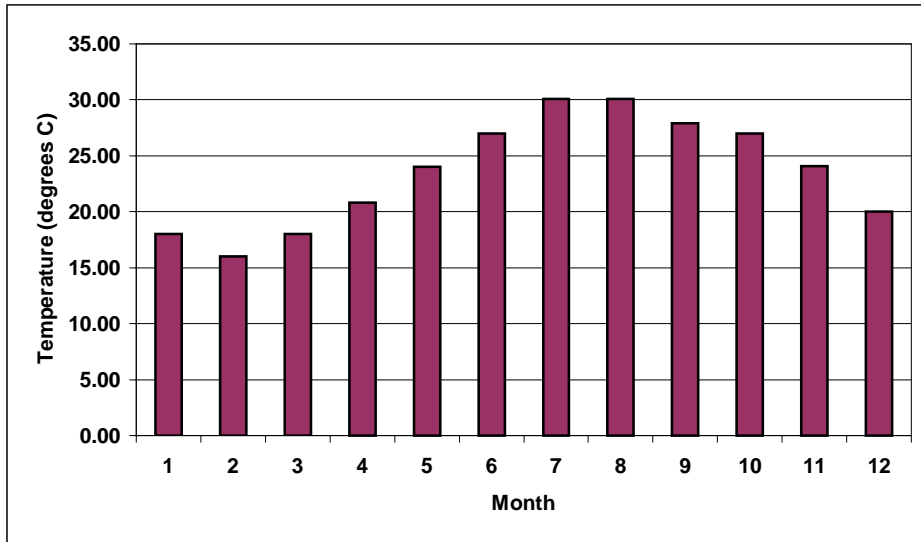


Figure 3. Estimated Mean Monthly Water Temperatures for WCA 3A-15. Estimated from HydroQual (1997).

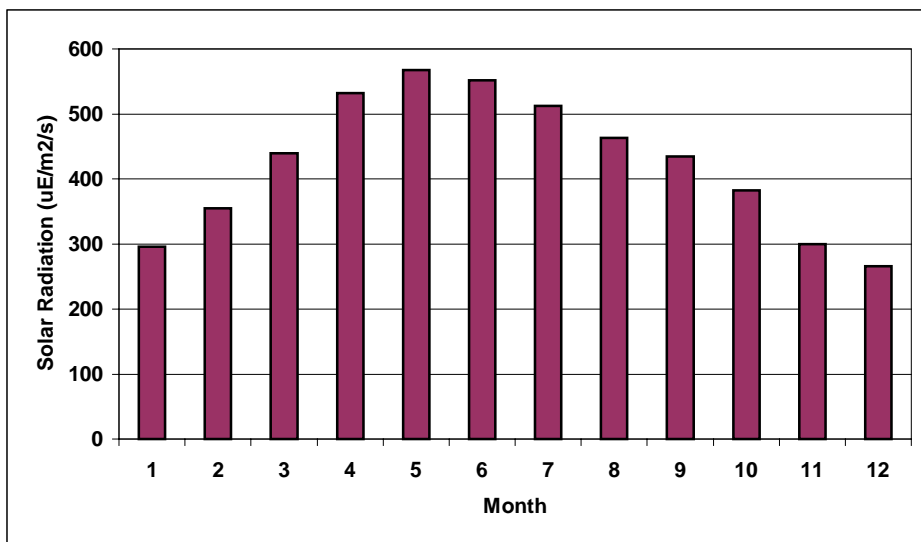


Figure 4. Mean Monthly Incident Light for WCA 3A-15. Source: Estimated from HydroQual (1997).

5.2.3 Hydrology

Precipitation data were averaged from three sites: FAMS data for Tamiami Trail (TT), Fakahatchee Strand (FS), and Andytown (AT) from 1992-96.

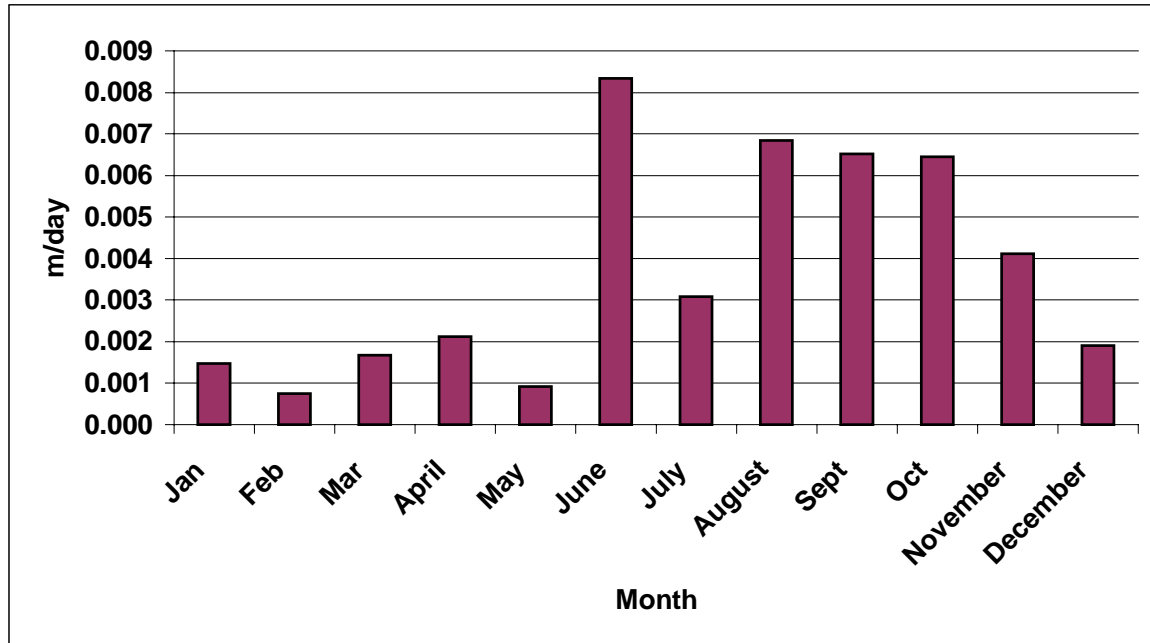


Figure 5. Estimated mean monthly precipitation for WCA 3A-15. Data from Everglades FAMS sites, 1992-1996. Source: Gill *et al.*, (1999).

Field data are lacking for the surface flowrates at WCA 3A-15. The following approach was therefore taken to estimate mean monthly surface flows:

- Assume cell size of interest: 1 km x 1 km, 0.5 m average depth for surface water;
- Assume hydraulic residence time: $\tau_w = 48$ days (similar to Ambrose *et al* 1997);
- Compute average annual flow and water velocity through cell based on hydraulic residence time;
- Compile average monthly precipitation from FAMS sites AT, FS, and TT for 1992-1996 (annual average = 134.6 cm);
- Assume seasonality of surface flow mimics precipitation;
- Scale mean monthly flows to match pattern of observed precipitation.

The result of the above exercise is shown in Figure 6. There are distinct dry and wet seasons in the winter and summer/fall respectively. Inflows were assumed equal to outflows.

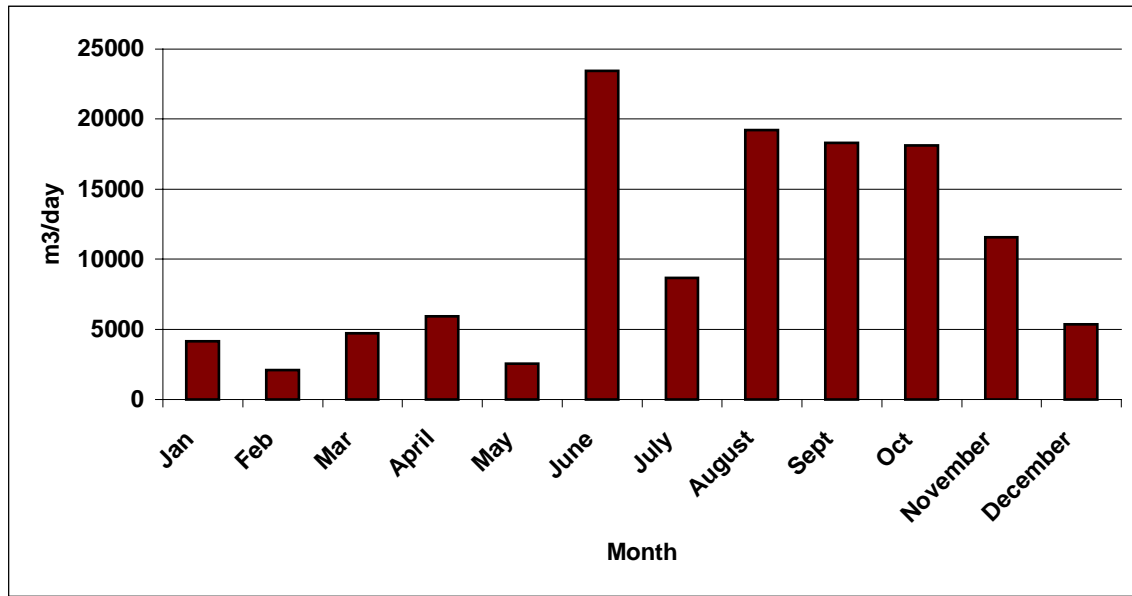


Figure 6. Estimated Mean Monthly Surface Inflows and Outflows for WCA 3A-15. Source:

Water depths were measured directly at WCA 3A-15 by the USGS, Miami Florida Sub District Office. Data for complete calendar years of daily data were available for 1996 and 1997 and were averaged to estimate daily water levels, shown in Figure 7.

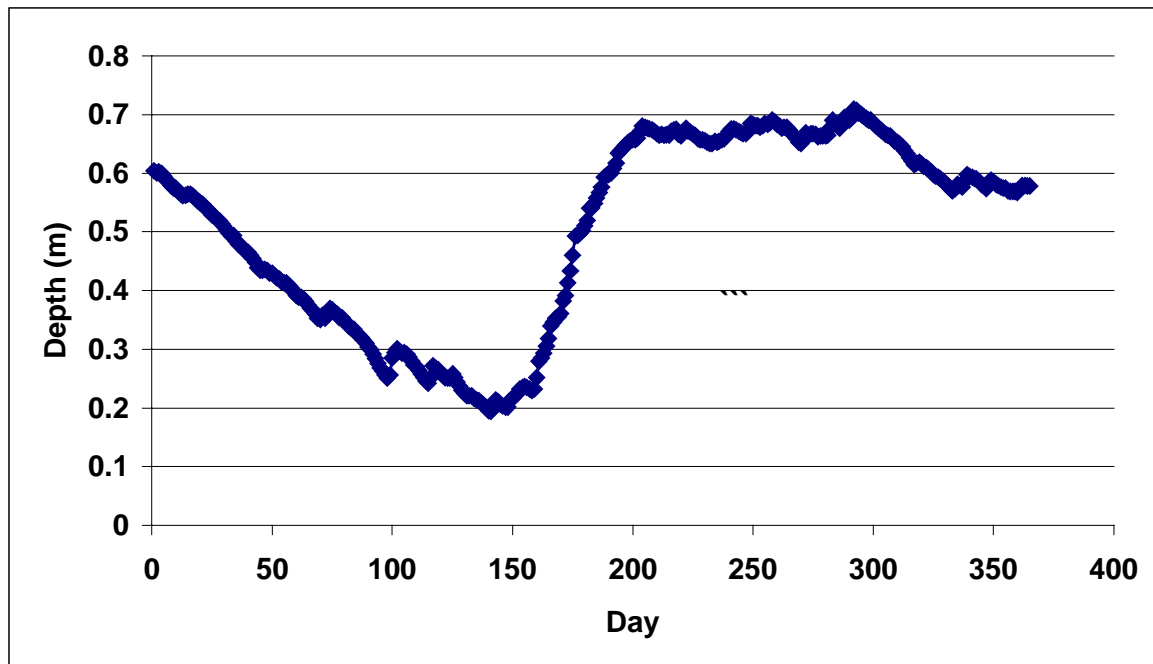


Figure 7. Estimated daily surface water depths for WCA 3A-15 (Source: 1996-97 ACME unpublished data)

5.2.4 External Mercury Loadings

Estimates of monthly wet, dry and RGM deposition rates for Hg(II) were provided by Keeler *et al.*, (2000), based on sampling undertaken between June 1995 and June 1996. The deposition rates used in the simulations with current atmospheric Hg(II) deposition are shown in Figures 8 and 9.

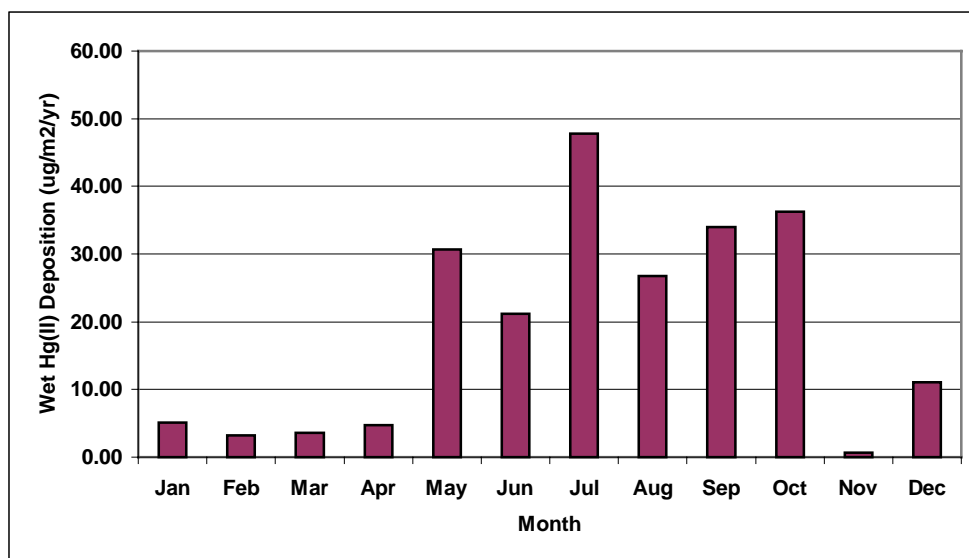


Figure 8. Monthly wet Hg(II) deposition rates used in long-term E-MCM calibration.
Source: 1995-1996 data from Keeler *et al.*, 2000)

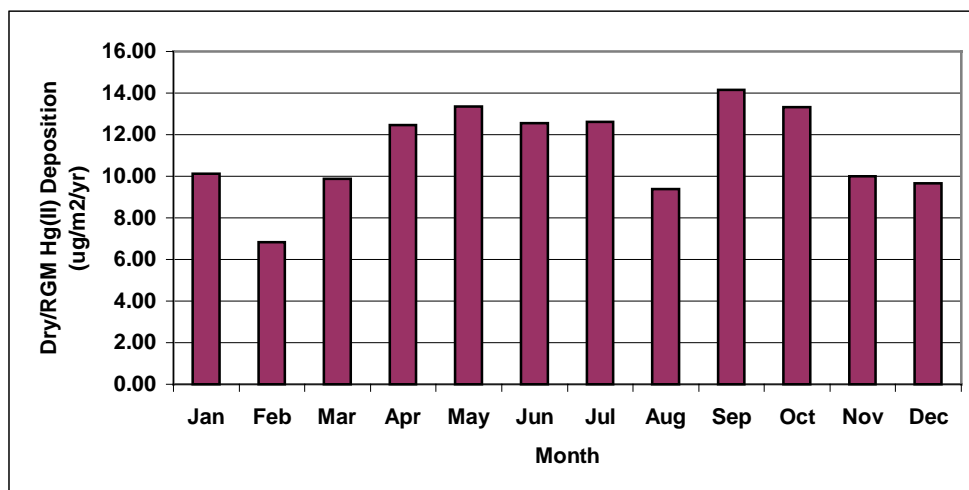


Figure 9. Monthly dry/RGM Hg(II) deposition rates used in long-term E-MCM calibration.
Source: 1995-1996 data from Keeler *et al.*, 2000)

Methylmercury concentrations in wet deposition were assumed to equal 0.15 ng/L. This concentration likely represents an upper limit; limited data collected during FAMS at several Everglades sites showed that methylmercury concentrations in monthly integrated bulk deposition samples were equal to or below 0.020 ng/L (Guentzel *et al.*, 1995). Sensitivity analyses demonstrate that the model is insensitive to variations in concentrations at these comparatively low levels. Dry deposition rates for methylmercury were assumed to be negligible.

The USGS ACME study collected surface water concentrations of total and methylmercury at several sites, including 2BS a location upstream of 3A-15. The average concentrations of Hg(II) and methylmercury were 2.32 and 0.46 ng L⁻¹ respectively for 9 sampling dates between July 1995 and June 1998. These concentrations were assumed to be the surface inflow concentrations for site 3A-15.

5.2.5 Water Chemistry Inputs

Several water quality parameters have been identified as having an impact on concentrations of total and methylmercury in freshwater systems. In particular, dissolved organic carbon, pH and chloride have received much attention. Table 5 shows the values used for these parameters during WCA 3A-15 simulations.

5.2.6 Food Web Inputs

The food web in the Everglades is complex. For the purposes of this study, a simplified nine-compartment food web was selected as shown in Figure 10. These compartments are anticipated to be those most involved in the transfer of methylmercury through the food web to our endpoint, largemouth bass.

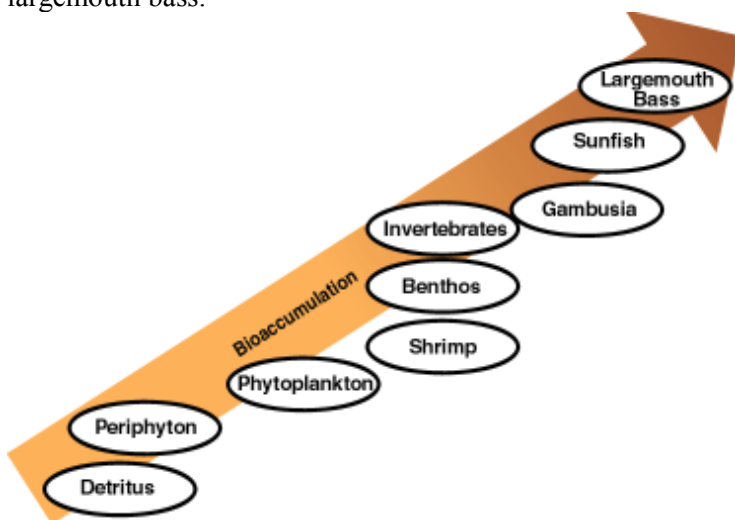


Figure 10. Food Web Compartments in E-MCM

In the above food web scheme, largemouth bass could eat any combination of food items desired from the other compartments. Bluegill and warmouth were combined as a single omnivorous fish category called sunfish, but could not eat largemouth bass. *Gambusia* were assumed not to eat other fish, relying instead on plankton, periphyton and benthos. Tables 7 through 9 and Figure 11 show the diets used in the E-MCM calibration for each of the three fish populations at different ages. These diets were developed based on discussions with ACME researchers investigating the food web on-site (L. Cleckner, P. Garrison, pers. comm.).

Dietary Item	Fraction of diet by wet weight for largemouth bass at different ages (years)							
	1	2	3	4	5	6	7	8
Periphyton	0.05	0.05						
Zooplankton	0.45	0.10	0.05	0.05				
Benthos	0.10	0.20	0.15	0.05	0.05	0.05	0.05	0.05
Shrimp	0.20	0.25	0.20	0.10	0.05	0.05	0.05	0.05
Piscivore							<0.01	<0.01
Fish	.2	.4	.6	0.80	0.90	0.90	0.90	0.90
Total	1	1	1	1	1	1	1	1

Table 7. Dietary pattern of largemouth bass used for final calibration

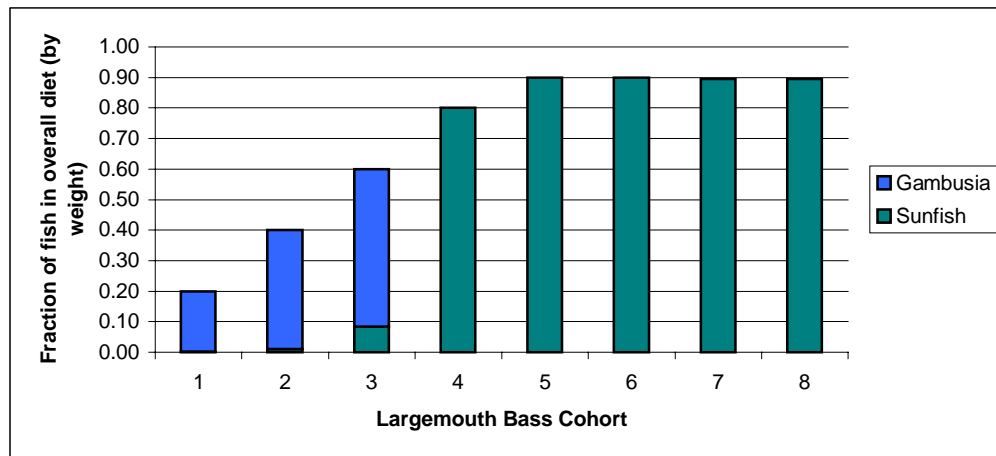


Figure 11. Fractions of largemouth bass diet (by weight) represented by *Gambusia* and Sunfish in final calibration.

Dietary item	Fraction of diet by wet weight for sunfish at different ages (years)					
	1	2	3	4	5	6
Phytoplankton	0.05	0.06				
Periphyton	0.15	0.22	0.07	0.05	0.05	0.05
Invertebrates	0.30	0.17	0.27	0.05	0.05	0.05
Benthos	0.25	0.28	0.33	0.30	0.30	0.30
Shrimp	0.25	0.28	0.33	0.30	0.30	0.30
<i>Gambusia</i>				0.30	0.30	0.30
Total	1	1	1	1	1	1

Table 8. Dietary pattern of sunfish used for final calibration.

Dietary Item	Fraction of diet on wet weight basis
Periphyton	0.25
Zooplankton	0.40
Benthos	0.25
Shrimp	0.10

Table 9. Dietary pattern of *Gambusia* used for final calibration.

Fish growth rates can also significantly affect mercury concentrations. Growth data provided by the Florida Department of Environmental Protection (T. Lange, unpublished data) were used for largemouth bass as shown in Figure 12.

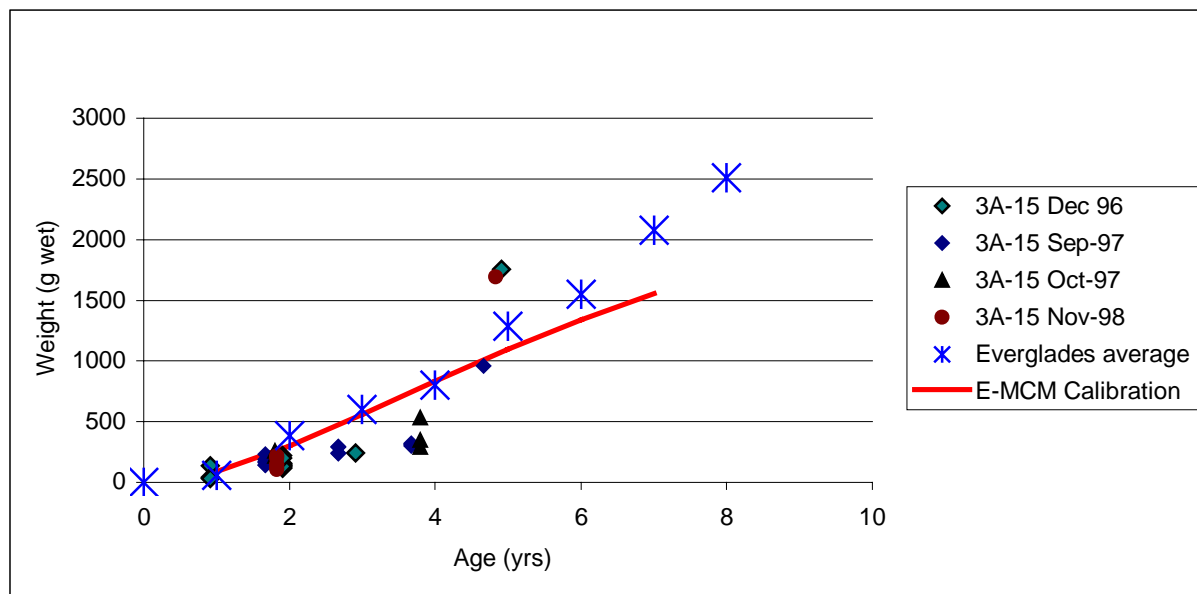


Figure 12. Observed and Calibrated Growth Rates for Largemouth Bass

The relationship between fish length and weight is also important in E-MCM since there is a preferred prey size range for piscivory, based on fish lengths. Data provided by the Florida Department of Environmental Protection (T. Lange, unpublished data) were used for largemouth bass as shown in Figure 13. Largemouth bass were assumed to prefer prey ranging from 15 to 40% of their own length. On occasions where sunfish were piscivorous, they were assumed to prefer fish ranging from 5 to 33% of their own length. These preferences resulted in largemouth bass and sunfish fish consumption patterns shown earlier in Tables 7 to 9.

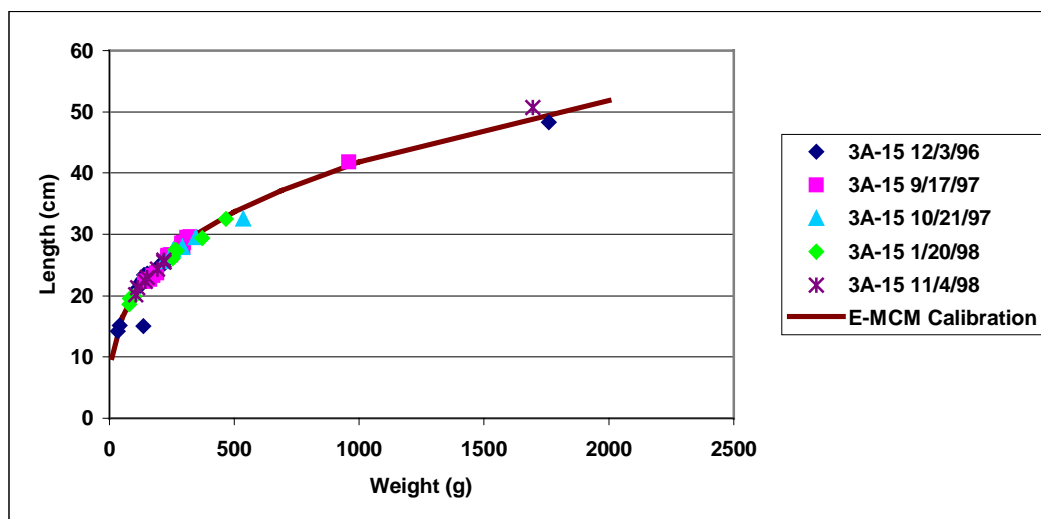


Figure 13. Length versus Weight relationship for Largemouth Bass at WCA 3A-15.

5.2.7 Particle Dynamics

Growth and turnover of vegetation such as sawgrass, cattails and lilies, settling, decomposition and burial of particles play an important role in mercury cycling in the Everglades (Ambrose *et al.*, 1997, this study). Table 10 shows mean annual values associated with E-MCM inputs for vegetation particle fluxes in the water column.

	Fraction of cell area covered by plant	Biomass		Turnover rate	Litter flux to sediment interface	Fraction mineralized at interface	Mass of particles entering sediments
Units:		g dry/m ² plant cover	g dry/m ² cell	1/yr	g dry/m ² /yr		g dry/m ² /yr
Source:	Assumed	Ambrose <i>et al.</i> , 1997	Calculated	Ambrose <i>et al.</i> , 1997	Calculated	Assumed	Calculated
Species:							
Sawgrass	0.27	572	154	2.08	321	0.1	289
Lilly	0.2	114	23	2.08	48	0.1	43
Cattail	0.03	700	21	4	84	0.1	76
Periphyton	0.75	360	270	2.2	594	0.1	535
Total			~468		1047		942

Table 10. Vegetation-related particle fluxes in the water column: E-MCM inputs

Figure 14 shows the particle budget calibrated for the surficial sediment layer (0-3 cm). The mean annual bulk burial velocity at the bottom of the surficial sediment layer (3cm) was 2.87 mm yr⁻¹.

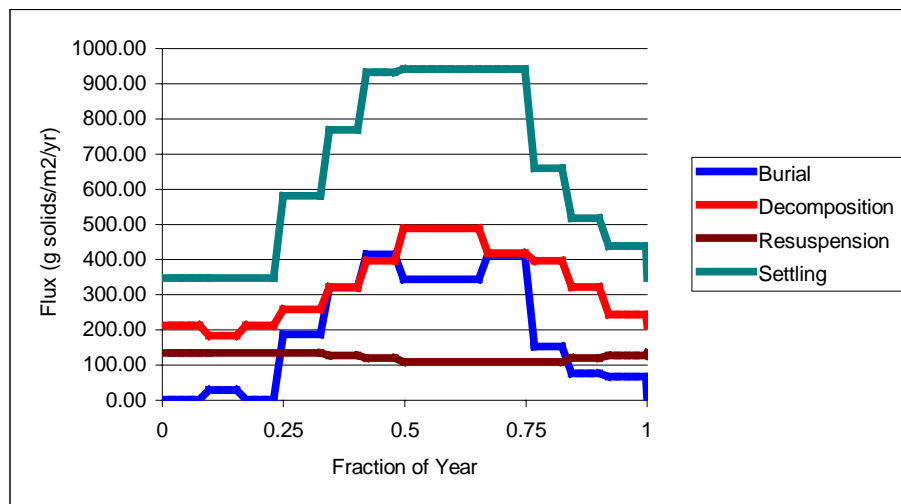


Figure 14. Calibrated particle fluxes for surficial sediments.

6. Results

6.1 Model Calibration to Current Loadings

The calibration of long-term average concentrations at WCA 3A-15 to the estimated current annual atmospheric Hg(II) deposition rate of $30.94 \mu\text{g m}^{-2} \text{yr}^{-1}$ (wet and dry deposition combined) are shown in Table 11 and Figures 15 through 20. Mercury observations in water and sediments are based on sampling programs from 1995-98 by the ACME research team (e.g. Krabbenhoft *et al.*, 1998, Gilmour *et al.*, 1998a, Hurley *et al.*, 1998, Cleckner *et al.*, 1998). Fish mercury observations by the Florida Department of Environmental Protection (T. Lange unpublished data) spanned a period from December 1996 through November 1998. Predicted long-term average concentrations were developed by running E-MCM for one hundred years with repeating annual cycles of site conditions and mercury loadings, to effectively reach a stable situation. The model was then run for one more year saving results on a weekly basis.

Table 11 shows observed and predicted mean concentrations for total mercury and methylmercury in surface waters and sediments at WCA 3A-15. Predicted concentrations of total and methylmercury in surface waters and sediments are within observed ranges for the most part (Figures 15 and 16).

Table 11. Comparison of Observed and Predicted Hg concentrations in Surface Waters and Sediments at WCA 3A-15				
Parameter	Units	Predicted Mean	Observed Mean	Observed Reference
Unfiltered total Hg in surface water	ng L ⁻¹	1.50	1.94 (n=8)	Krabbenhoft <i>et al.</i> , (unpublished data)
Unfiltered MeHg in surface water	ng L ⁻¹	0.61	0.50 (n=8)	Krabbenhoft <i>et al.</i> , (unpublished data)
Total Hg on sediment solids (observed = 0-2 cm; predicted = 0-3 cm)	ug g ⁻¹ dry	0.12	0.114 (n=5)	Gilmour <i>et al.</i> , (1998b)
MeHg on sediment solids (observed = 0-2 cm; predicted = 0-3 cm)	ug g ⁻¹ dry	0.003	0.004 (n=5)	Gilmour <i>et al.</i> , (1998b)

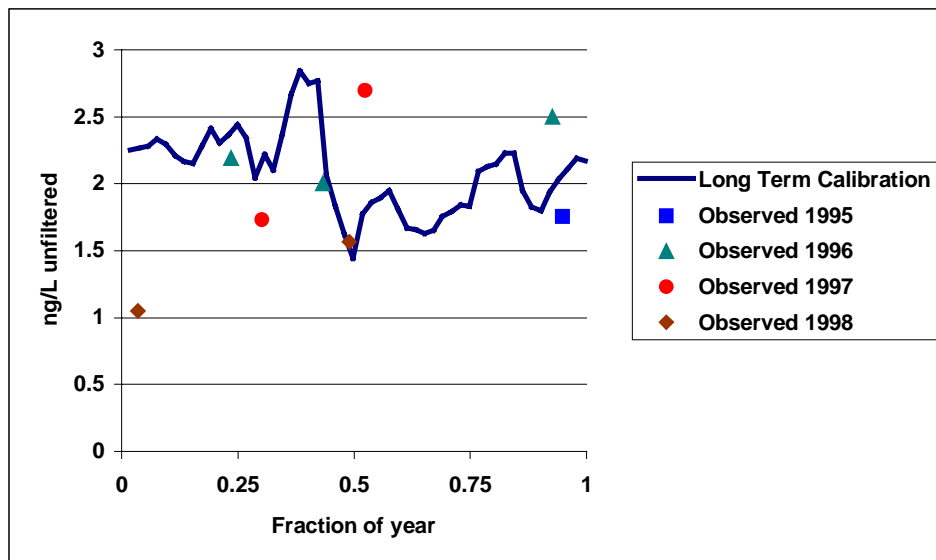


Figure 15. Predicted long-term concentrations of total mercury in WCA 3A-15 surface waters for calibration with current atmospheric Hg(II) deposition = 30.94 $\mu\text{g}/\text{m}^2/\text{yr}$. Observations: Krabbenhoft *et al.*, (**unpublished data**)

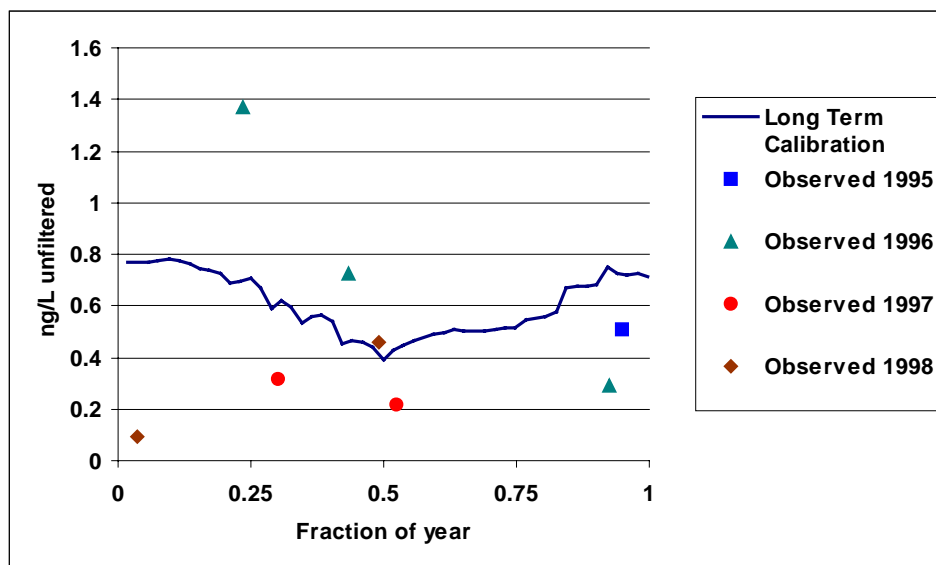


Figure 16. Predicted long-term methylmercury concentrations in WCA 3A-15 surface waters for calibration with current atmospheric Hg(II) deposition = 30.94 $\mu\text{g}/\text{m}^2/\text{yr}$. Observations: Krabbenhoft *et al.*, (**unpublished data**)

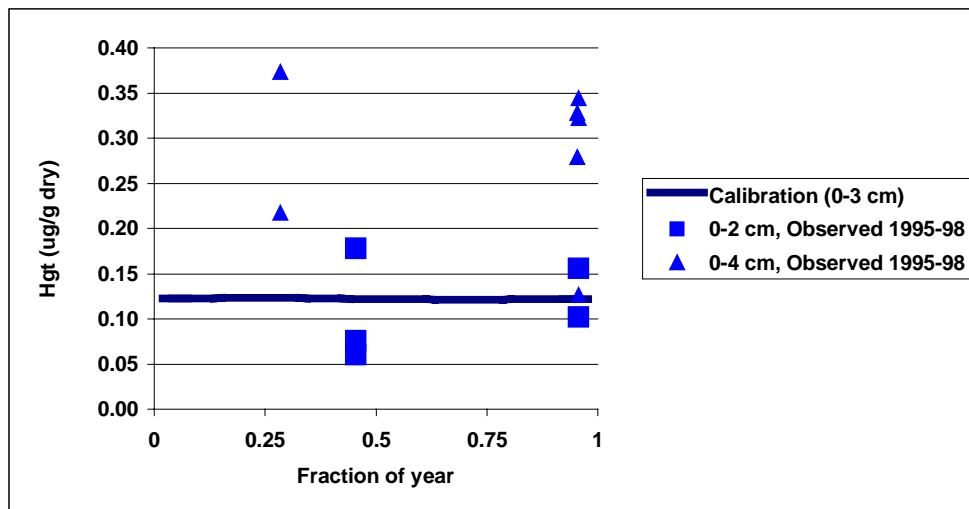


Figure 17. Predicted long-term Hgt concentrations in WCA 3A-15 surface sediments for calibration with current atmospheric Hg(II) deposition = 30.94 $\mu\text{g}/\text{m}^2/\text{yr}$. Observations: Gilmour *et al.*, 1998b

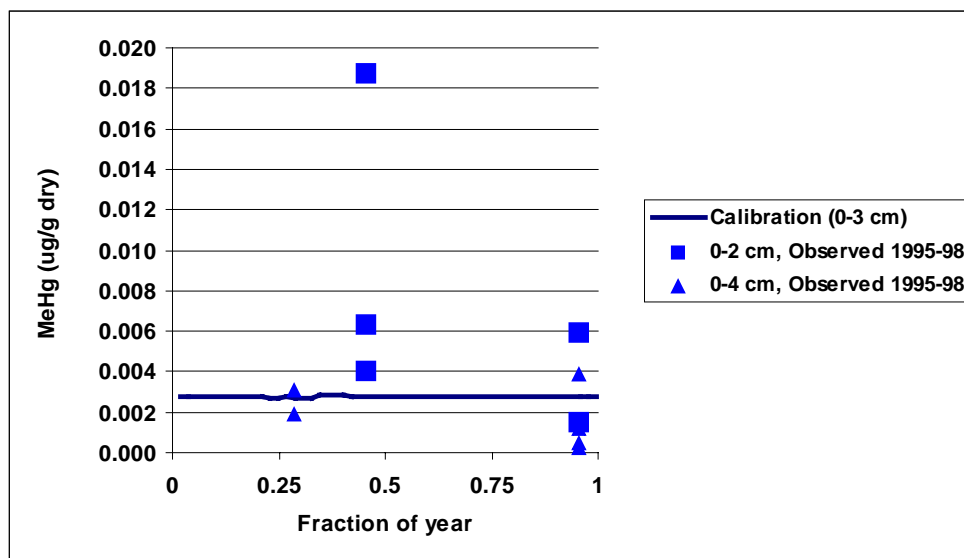


Figure 18. Predicted long-term MeHg concentrations in WCA 3A-15 surface sediments for calibration with current atmospheric Hg(II) deposition = 30.94 $\mu\text{g}/\text{m}^2/\text{yr}$. Observations: Gilmour *et al.*, 1998b

Predicted mercury concentrations for *Gambusia*, sunfish and largemouth bass were also consistent in magnitude with observations. Predicted *Gambusia* mercury concentrations were 0.13 and 0.23 $\mu\text{g}/\text{g}$ wet whole body at age 3 months and 6 months respectively. Mean values reported for 3 sampling periods in 1997 to 1998 ranged from 0.057 to 0.166 $\mu\text{g}/\text{g}$ wet whole body (D. Krabbenhoft, unpublished data). Predicted and observed mercury concentrations for warmouth, bluegill and largemouth bass are shown in Figures 19 and 20. The model has three fish populations: non-piscivores, omnivores and piscivores. Bluegill and warmouth were treated as a single omnivorous fish type, referred to generically as sunfish. The calibration predicted

sunfish concentrations well (Figure 19). Mercury concentrations in largemouth bass were reasonably predicted (Figure 20) although the model predicted increasing concentrations with size, while the observations show an unusual pattern. Between 15 to 30 cm lengths, largemouth bass mercury concentrations show no obvious increase, and range from approximately 0.5 to 1.5 $\mu\text{g g}^{-1}$ wet muscle. Beyond a length of 35 cm (approximately age 3), there are few observations (n=3) but the values are all equal or greater than 3.0 $\mu\text{g g}^{-1}$ wet muscle.

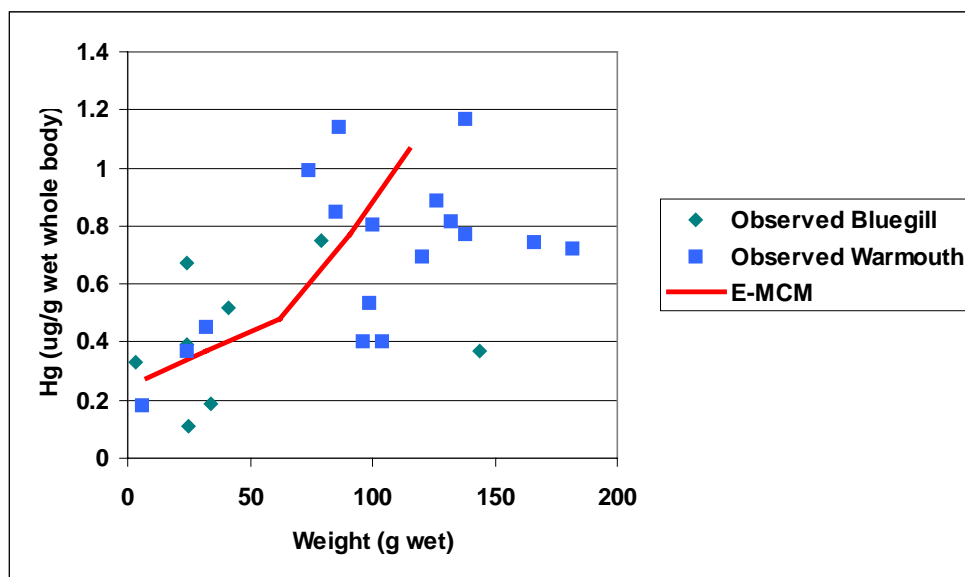


Figure 19. Predicted long-term methylmercury concentrations in sunfish in WCA 3A-15 for calibration with current atmospheric Hg(II) deposition = 30.94 $\mu\text{g/m}^2/\text{yr}$. Observations: Lange *et al.*, unpublished data

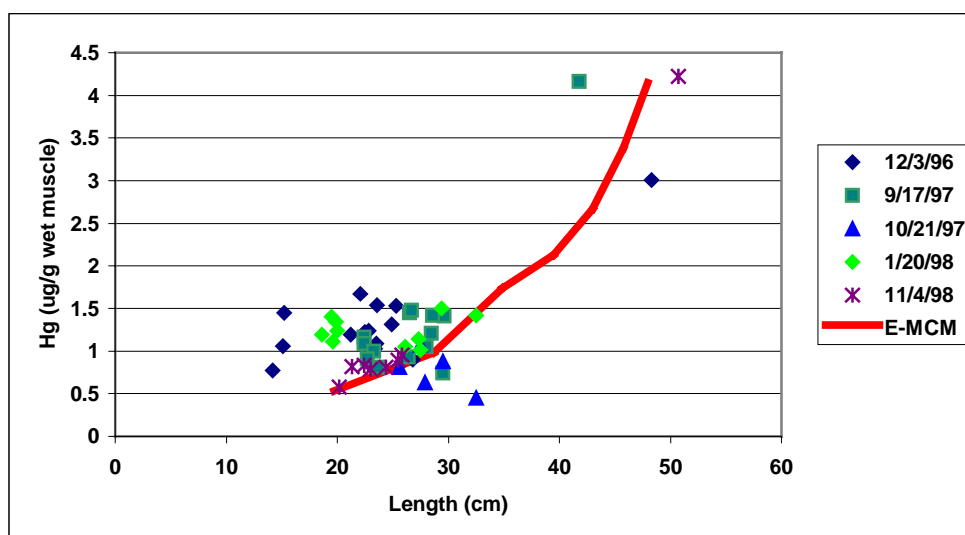


Figure 20. Predicted long-term methylmercury concentrations in largemouth bass in WCA 3A-15 for calibration with current atmospheric Hg(II) deposition = 30.94 $\mu\text{g/m}^2/\text{yr}$. Observations: Lange *et al.*, unpublished data

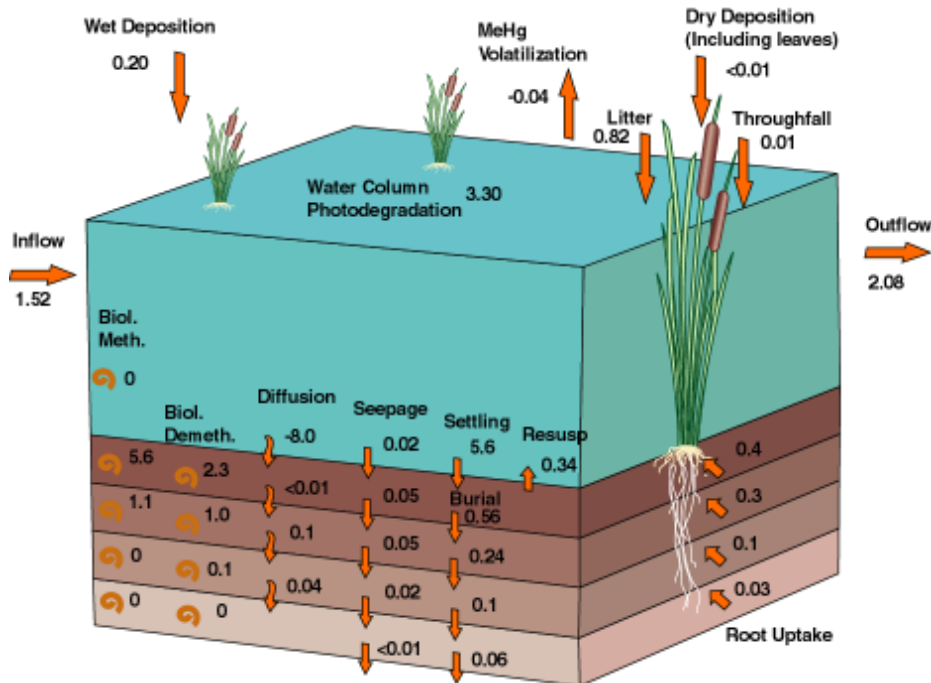


Figure 22. Predicted long-term annual MeHg fluxes $\mu\text{g m}^{-2} \text{yr}^{-1}$ for calibration to annual atmospheric Hg(II) deposition rate of $30.94 \mu\text{g m}^{-2} \text{yr}^{-1}$

6.2 Long-term Hg(II) Deposition – Fish Hg Response Curve

A fundamental question to examine in this pilot TMDL study was the relationship between atmospheric Hg(II) deposition and long-term fish mercury concentrations. Once the model was calibrated to the current atmospheric Hg(II) deposition estimate of $30.94 \mu\text{g m}^{-2} \text{yr}^{-1}$, simulations were also carried out with loadings at 75, 50, 25 and 15% of current levels. In these simulations, HgII and methylmercury concentrations in inflows were adjusted in proportion to Hg(II) deposition, but atmospheric methylmercury deposition was not changed. Predicted fish mercury concentrations were compared after each simulation had run 100 years using repeating annual cycles of site conditions and mercury deposition.

Figure 23 shows the predicted long-term relationship between atmospheric mercury deposition and mercury concentrations in age 3 largemouth bass in WCA 3A-15

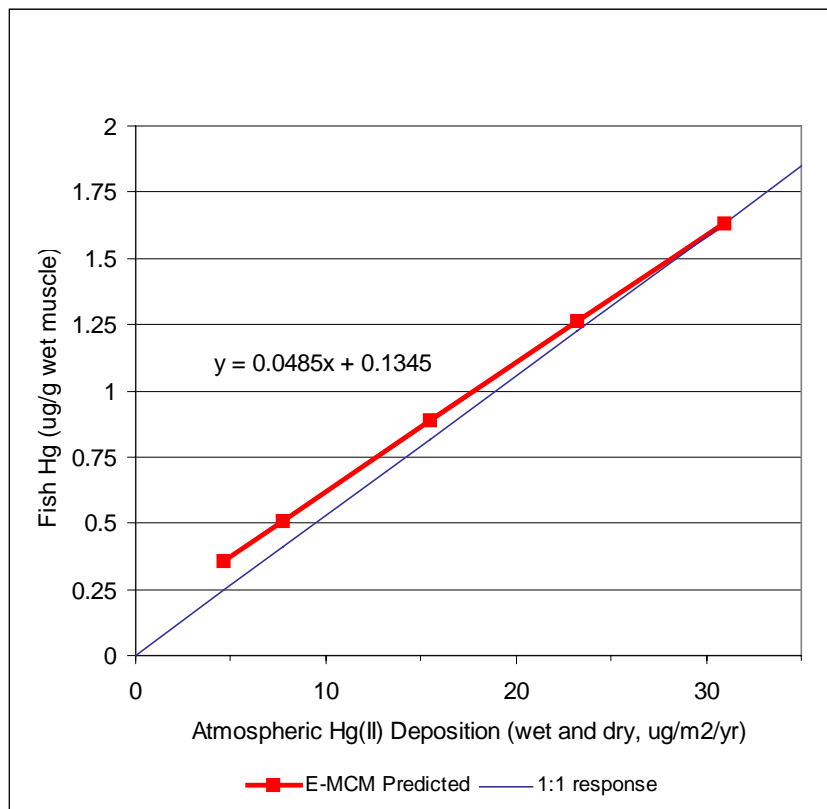


Figure 23. Predicted Hg concentrations in age 3 largemouth bass as a function of different long-term constant annual rates of wet and dry Hg(II) deposition. Predictions are based on calibration to current loading of $30.94 \mu\text{g m}^{-1} \text{yr}^{-1}$.

Figure 24 is based on the same modeling results as Figure 23, but presents information as fractions of current fish mercury concentrations and atmospheric Hg(II) deposition. A linear relationship is predicted, but the slope is not 1.0 and the intercept in both Figures 23 and 24 is non-zero. This indicates that there is not an exact correspondence between relative reductions in Hg(II) loading and fish Hg response. Furthermore, in the absence of any Hg(II) loading from any sources, there will still be some mercury accumulating in largemouth bass. This latter consequence can occur only if sources other than atmospheric inputs of Hg(II) become important. And indeed this is the case: we assumed as an input to E-MCM some (albeit minor) atmospheric loadings of methylmercury to the system which are unaffected by changes in Hg(II) deposition. This methylmercury source takes on greater importance when other methylmercury sources are reduced.

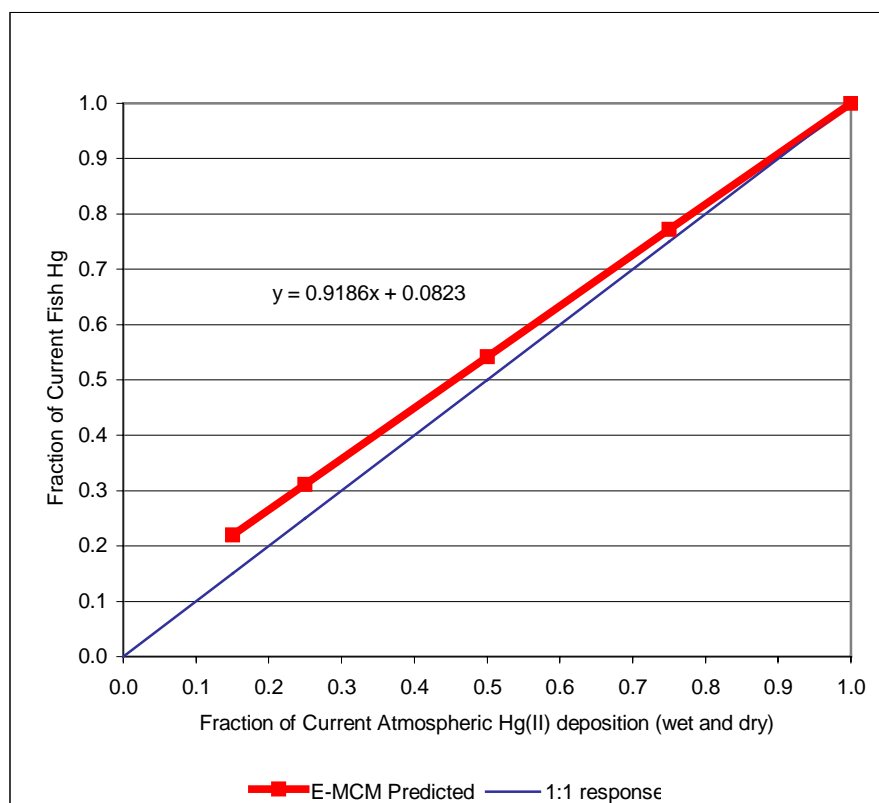


Figure 24. Predicted fraction of current Hg concentration in age 3 largemouth bass as a function of long-term reductions in Hg(II) deposition (wet and dry). Predictions are based on calibration to current loading of $30.94 \mu\text{g m}^{-1} \text{yr}^{-1}$.

6.3 Timing of the System Response

A second fundamental question of the pilot Hg TMDL exercise was: How fast will fish mercury concentrations change following reductions in Hg loading? We examined this question by running simulations for 200 years to reach steady state and then instantaneously reducing atmospheric deposition in a step function manner and continuing the simulation for an additional 200 years. The results for load reductions of 25, 50, 75 and 85% from the current deposition estimate of $30.94 \mu\text{g m}^{-1} \text{yr}^{-1}$ are shown in Figure 25.

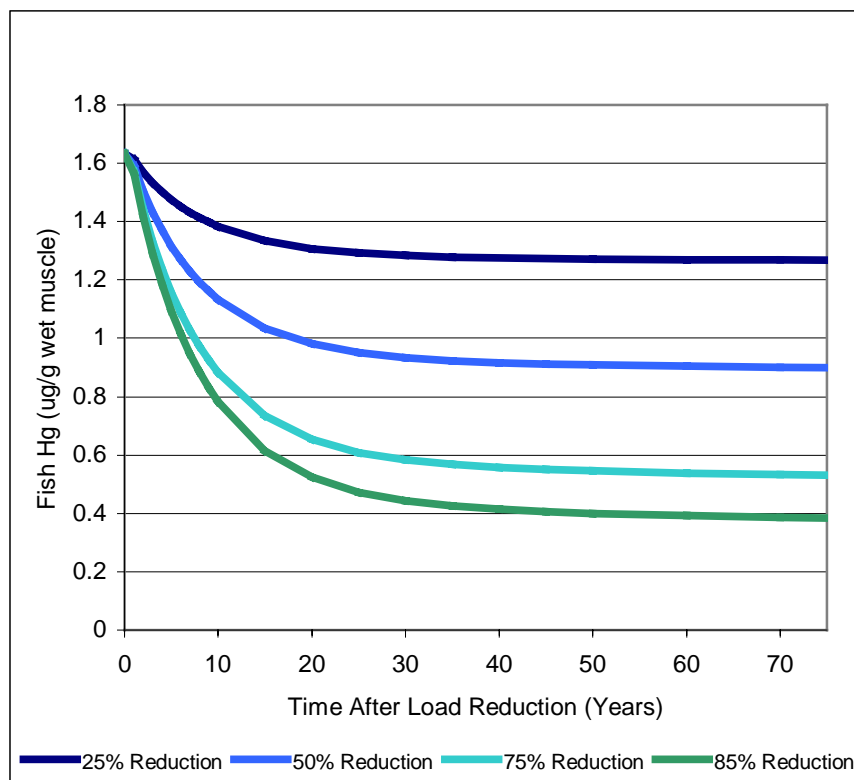


Figure 25. Predicted dynamic response of Hg concentrations in largemouth bass in WCA 3A-15 following different reductions in Hg(II) deposition. Predictions are based on calibration to current loading of $30.94 \mu\text{g m}^{-1} \text{yr}^{-1}$.

We also wanted to test whether the rate at which fish mercury concentrations approached a new steady state situation following a load reduction depended on the magnitude of the load change. Figure 26 shows that the number of years for the system to approach a new steady state is effectively independent of the actual magnitude of the change. For example, the numbers of years predicted to achieve 50% of the ultimate response in fish Hg is approximately 6 to 7 years, for all load reduction scenarios tested with the base calibration with atmospheric Hg(II) deposition = $30.94 \mu\text{g m}^{-2} \text{yr}^{-1}$. For comparative purposes, Figure 26 also shows a curve for a simple exponential approach to steady state ($y = 1 - e^{-kt}$, $k = 0.11$, $t = \text{years}$). The simple exponential curve fits the model predictions well initially but there is a slower 2nd phase response after 20 years.

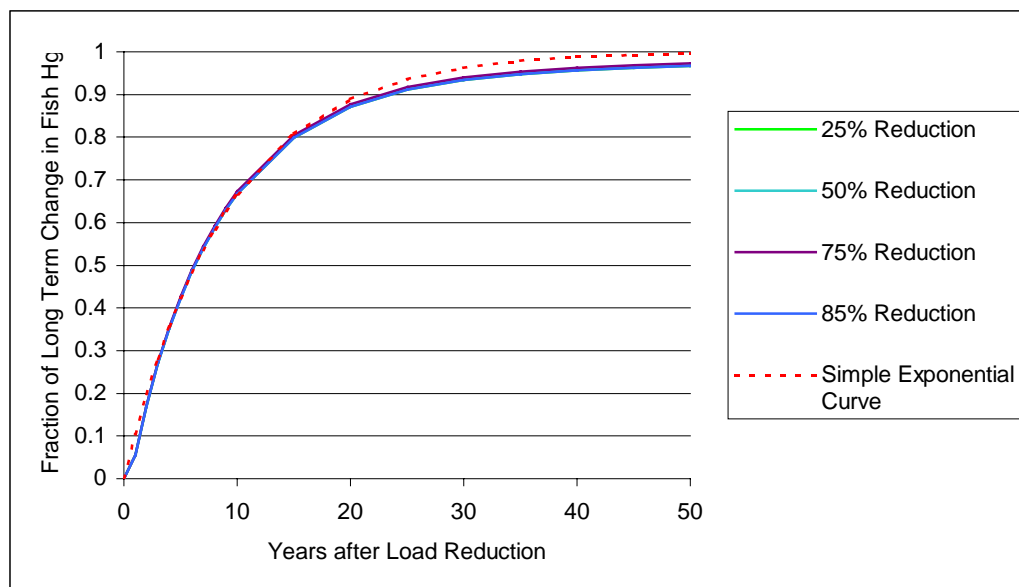


Figure 26. Comparison of the rate at which age 3 largemouth bass concentrations approach steady state following different reductions in Hg(II) deposition (simulations all based on calibration with current Hg(II) deposition = $30.94 \mu\text{g m}^{-2} \text{yr}^{-1}$)

6.4 Sensitivity Analysis

It is important to understand which variables most affect predicted fish mercury concentrations in E-MCM at WCA 3A-15. Simulations were run varying inputs in isolation by a given amount, for example plus and minus 50%. In cases where a 50% change did not make physical sense, a lesser change was made, e.g. 10% or 25%. In addition, there were some inputs such as the fraction of fish in the diet that did not make sense to change in isolation. The following simultaneous changes were simulated:

- ❑ Fish growth rates and spawning sizes for all fish species were changed by the same percentage simultaneously.
- ❑ The areal coverage of the three macrophyte species, periphyton coverage and quantities of suspended solids and detrital material in the water column were varied simultaneously. It is expected that a change in vegetation cover would affect the amount of settling material. Burial rates were affected by these changes, since burial is calculated on the basis of sources and sinks of particulate matter to the sediments.
- ❑ When the diet of largemouth bass was altered to increase or decrease the fraction of fish in the diet, it was necessary to also alter the fractions of the diet represented by other food items. The fractions added or subtracted from fish consumption were distributed evenly amongst other food items.
- ❑ Surface inflow and outflow rates (Q_{in} and Q_{out}) were varied simultaneously since it was assumed these rates were equal in simulations.

- When atmospheric Hg(II) deposition was altered, we also altered surface inflowing Hg(II) and MeHg loads proportionately. Atmospheric methylmercury deposition was not altered.

To provide a common basis for comparing the effects of changes to inputs on fish Hg, results are presented as absolute value of ratio of the percent change in fish Hg divided by the percent change in the input:

$$|\% \text{ change in fish Hg}| / |\% \text{ change in input value}|$$

Mercury in age 3 largemouth bass was used as the end point of interest. Results of the sensitivity analysis are shown in Figure 27.

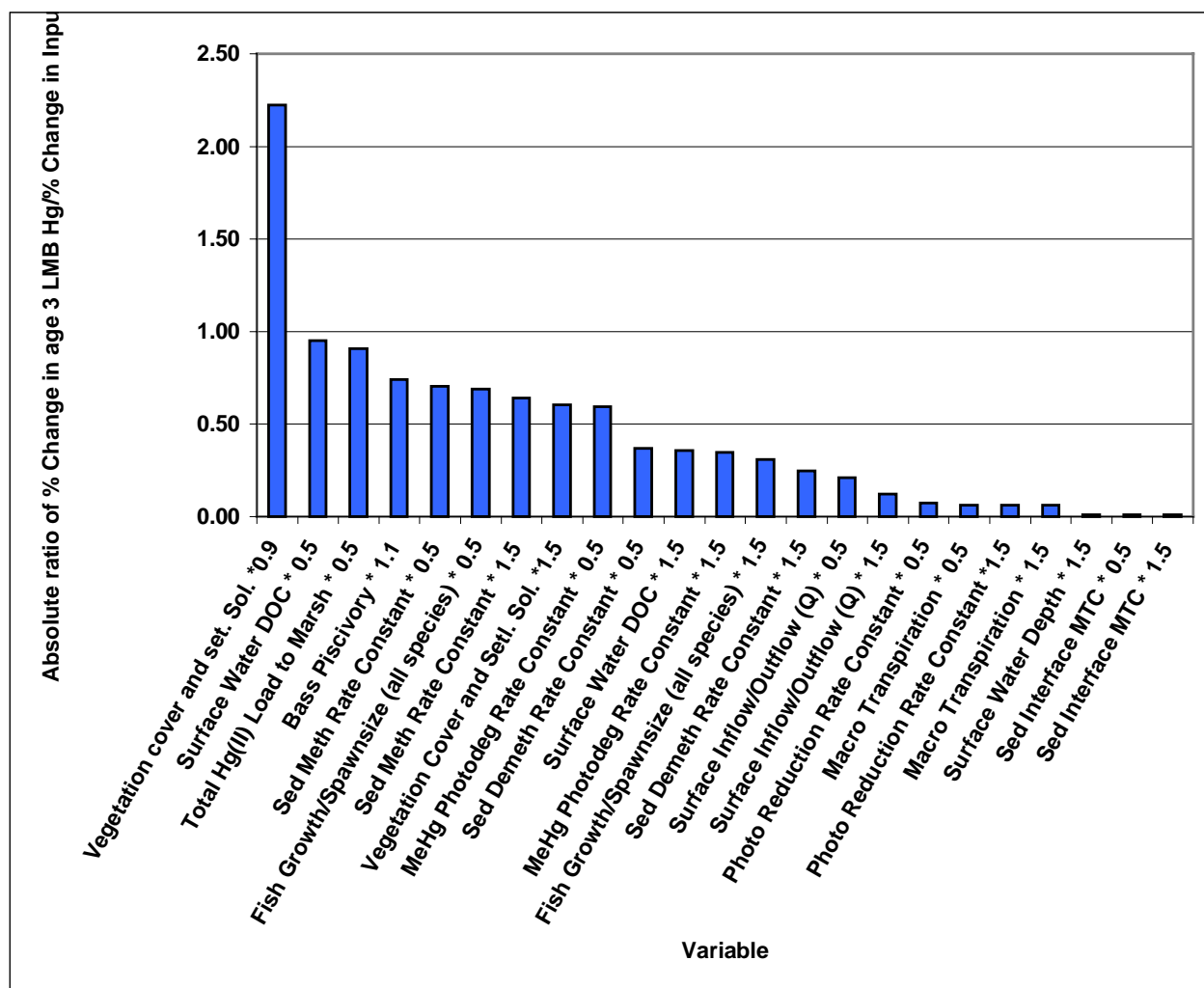


Figure 27. Predicted sensitivity of age 3 largemouth bass mercury concentrations in WCA 3A-15 to changes in various input values. Results are based on calibration with current atmospheric Hg(II) deposition = 30.94 $\mu\text{g}/\text{m}^2/\text{yr}$.

Predicted mercury concentrations in age 3 largemouth bass were most sensitive to factors associated with particle and vegetation fluxes, Hg(II) loading, methylation rates, and factors affecting fish diets and growth.

6.5 Year-to-Year Variability in Atmospheric Hg(II) Deposition

To address year-to-year variations in atmospheric Hg(II) deposition, we synthesized a set of 500 annual Hg(II) deposition rates as discussed in Section 4.5. A simulation was run for 200 years with a constant annual deposition rate ($30.94 \mu\text{g m}^{-1} \text{yr}^{-1}$), and then continued for an additional 500 years with year to year variations in the total (wet and dry) atmospheric deposition rate. Figure 28 shows the distribution of annual deposition rates used in the simulation. A description of the development of this lognormal distribution is provided in Section 4.5.

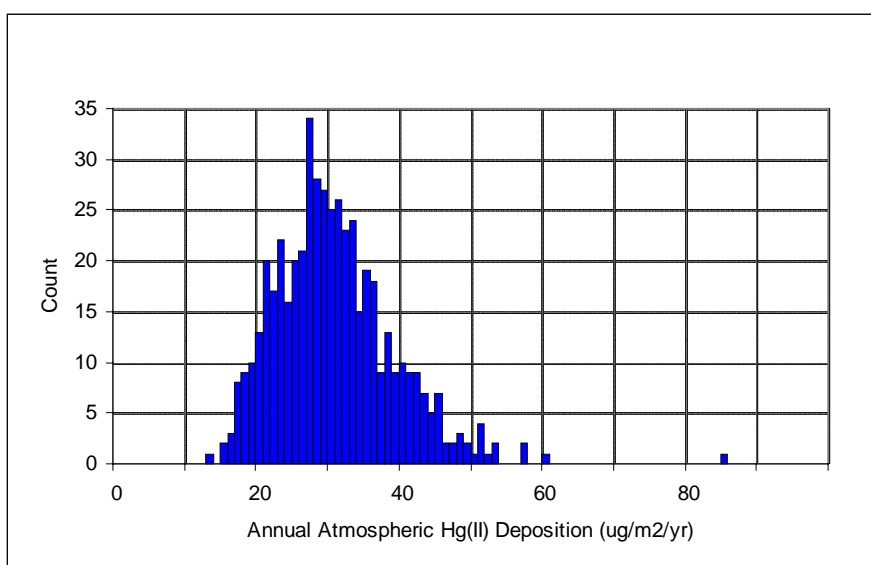


Figure 28. Distribution of annual atmospheric deposition rates used for 500 year simulation. Distribution synthesized from FAMS data as described in Section 4.5.

The results of the 500 year simulation are shown in Figure 29. Concentrations in age 3 largemouth bass varied from a low of $1.45 \mu\text{g g}^{-1}$ wet muscle to a high of $1.90 \mu\text{g g}^{-1}$ wet muscle. The mean concentration for the distribution was $1.64 \mu\text{g g}^{-1}$ wet muscle.

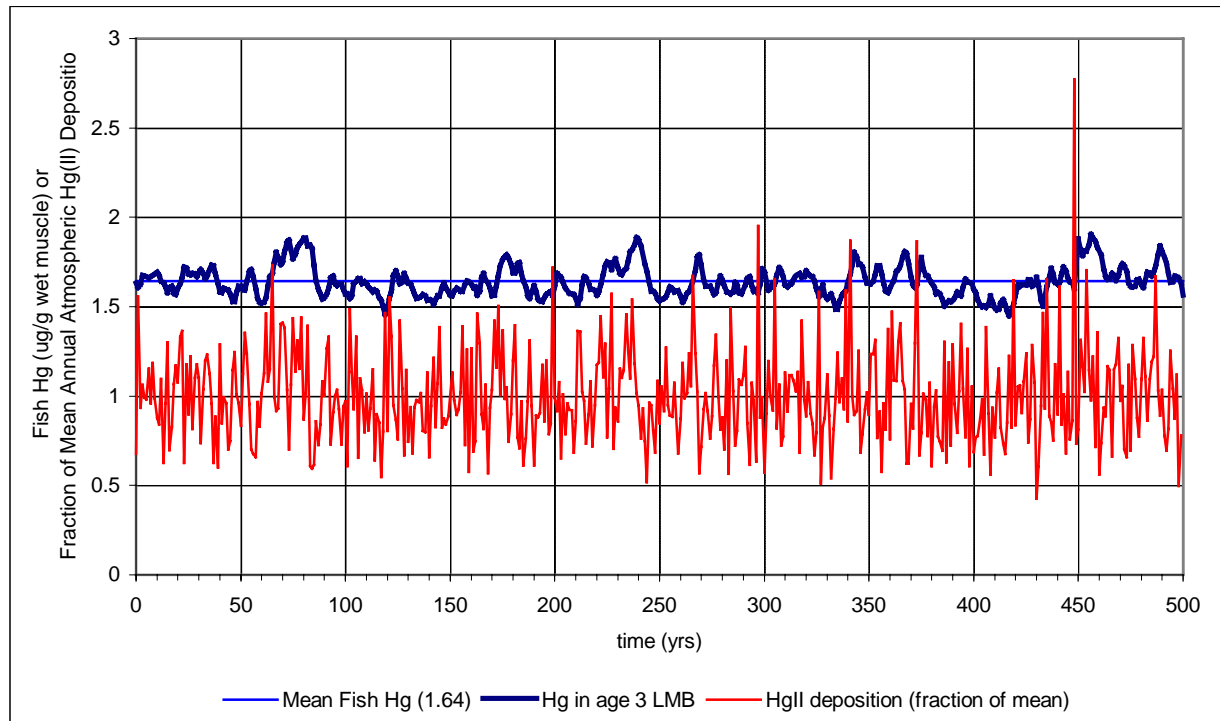


Figure 29. Input annual atmospheric Hg(II) deposition rates and predicted Hg concentrations in age 3 largemouth bass for 500 year simulation.

Figure 30 shows the distribution of predicted fish mercury concentrations for the 500 year simulation. Table 12 presents synoptic statistics for the distribution of 500 predicted fish mercury concentrations for age 3 largemouth bass.

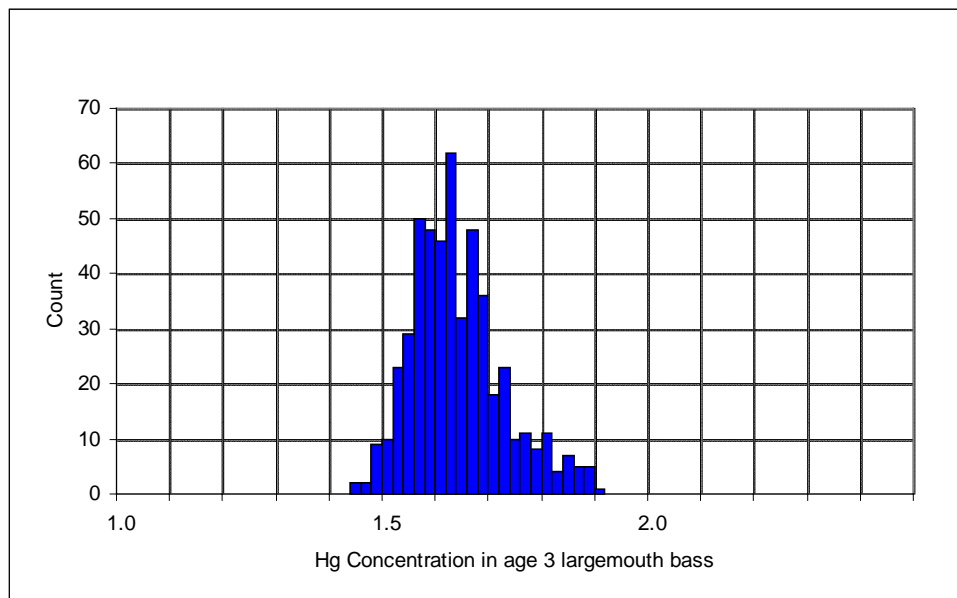


Figure 30. Distribution of predicted Hg concentrations in age 4.75 largemouth bass for 500 year simulation. Bin size = 0.02 $\mu\text{g/g}$.

Table 12. Summary Statistics for predicted Hg concentrations in age 3 largemouth bass for 500 year simulation ($\mu\text{g g}^{-1}$ wet muscle)	
Statistic	Value
Mean	1.64
Standard Error	0.0038
Median	1.63
Mode	1.58
Standard Deviation	0.0862
Sample Variance	0.0074
Kurtosis	0.2976
Skewness	0.6849
Range	0.45
Minimum	1.45
Maximum	1.90
Sum	820.77
Count	500

6.6 Uncertainty Regarding the True Current Rate of Atmospheric Hg(II) Deposition

There is uncertainty in the true current rate of atmospheric Hg(II) deposition, as discussed in Section 4.6. We calibrated the model to three different loads: 25.14, 30.94, and 36.74 $\mu\text{g m}^{-2} \text{yr}^{-1}$. In each case, model constants were adjusted for the given load to best match current concentrations measured in the system. As a measure of the effects of uncertain loading rates on our model results, we ran simulations for different loading reductions for each of the three calibrations. Figure 31 shows that the uncertainty regarding the true loading rate has little effect on the timing or magnitude of the response of age 3 largemouth bass to load reductions of 50%. Results were similar for load reductions of 15% and 75%.

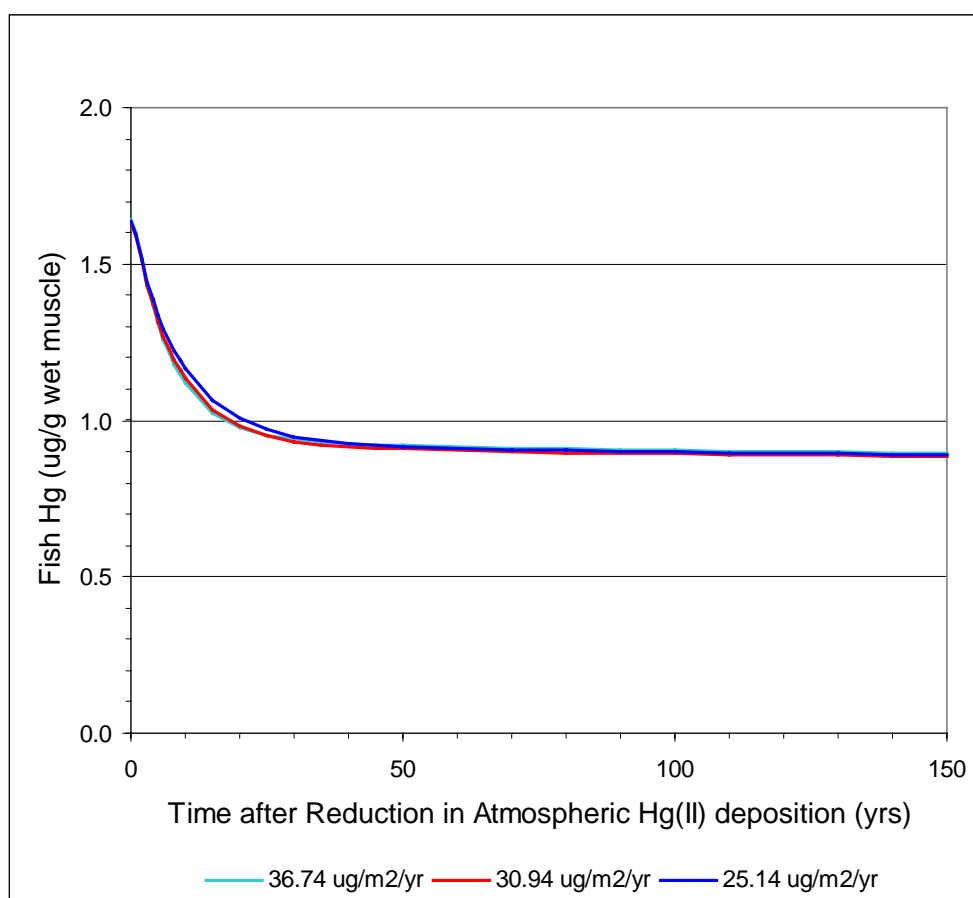


Figure 31. Predicted dynamic response of Age 3 LMB concentrations to a 50% reduction in Atmospheric Hg(II) deposition. Results are shown for three calibrations. Each calibration assumes a different current rate of deposition.

7. Discussion

7.1 Predicted Mercury Concentrations

Predicted surface water concentrations of total and methylmercury were very dynamic, capable of changing significantly within days. Field data show surface water mercury concentrations in fact to be capable of changing significantly on a within-day basis (Krabbenhof et al 1998), although simulations on this short a time scale were not undertaken during this study. Figures 15 and 16 indicate the long-term average model calibration is reasonably predicting the magnitude of observed concentrations of total and methylmercury in surface waters at WCA 3A-15. Since surface water Hg concentrations are very dynamic and responsive to recent site conditions and Hg loading patterns, it was not expected that the simulations of long-term average conditions (typically with inputs entered on a monthly basis) would match precisely the observations on specific dates sampled from 1995-98.

Observed concentrations of total and methylmercury in surface waters at WCA 3A-15 tend to be higher in the wet season (summer/fall) and lower in the dry season (winter) (D. Krabbenhof, pers. comm.). E-MCM predictions suggested slightly lower concentrations of total mercury in surface waters in the wet season however. This result was significantly influenced by the assumed seasonality of macrophyte litter production that resulted in increased scavenging of mercury from the water column in the wet season. In view of the discrepancy between observed and predicted seasonal trends for mercury in surface waters, the seasonality of vegetation biomasses and turnover rates should be reassessed in future work.

Predicted concentrations of total and methylmercury in surficial sediments (0-3 cm) also reasonably reflected observations (Figures 17 and 18). Significant variability existed for mercury concentrations in cores sampled on different dates and even for cores sampled on the same dates. Given the expertise of the field teams, this variability is likely real and due to natural variations between cores.

Observations of methylmercury concentrations in the lower food web (zooplankton, shrimp, periphyton, benthos) were limited but when combined with observed dietary patterns in fish, reasonable concentrations were predicted for *Gambusia*, sunfish and largemouth bass (Figures 19 and 20). *Gambusia* predictions are treated as tentative because:

- ❑ We did not find bioenergetics information specific to *Gambusia* for our simulations. We therefore used bioenergetics information for finescale dace.
- ❑ We did not have information on the growth rates for *Gambusia* at WCA 3A-15. Thus a growth rate pattern was assumed.
- ❑ *Gambusia* populations spawn several times during a 12 month period. E-MCM can only having spawning once per year, and is not set up for multiple cohorts within a year.

Thus while the predicted *Gambusia* concentrations were of the correct order of magnitude, we believe additional efforts are needed to locate literature values or measure *Gambusia* bioenergetics and growth rate information in the field/laboratory.

Good data were available for mercury concentrations in bluegill and warmouth at WCA 3A-15. As mentioned earlier, E-MCM has three fish populations so we combined bluegill and warmouth into a single omnivore category called sunfish. Table 8 shows the assumed sunfish dietary pattern which was primarily invertebrates, shrimp and benthos from ages zero to three, with some piscivory occurring at ages 4 and higher. Figure 19 shows a reasonable agreement between observations and predictions. Many of the warmouth observations exceeded $0.5 \mu\text{g g}^{-1}$ whole body, and would likely be even higher if determined on a muscle basis.

Predicted largemouth bass mercury concentrations in the long-term average simulations also agreed reasonably with observations (Figure 20), but the field dataset had some unexpected features. Most noticeably, there was little change in observed mercury concentrations between 15-30 cm fish. Concentrations in this length range were typically in the 0.5 to $1.5 \mu\text{g g}^{-1}$ wet muscle range. Beyond 35 cm in length, there were few observations ($n=3$) but the concentrations increased rapidly and were at or above $3 \mu\text{g g}^{-1}$ wet muscle in all cases. We achieved this result when the largemouth switched from eating primarily *Gambusia* to sunfish above age 3. This is consistent with field observations indicating largemouth bass switch from a low-mercury, mainly invertebrate diet to a high-mercury fish diet between ages 3 and 4 (T. Lange, pers. comm.).

Figure 29 suggests that if the annual variability in Hg(II) deposition at WCA 3A-15 is approximated by the FAMS dataset characteristics, the concentration exceeded 5% of the years would be $1.81 \mu\text{g g}^{-1}$ wet muscle ($=1.64 + (1.96*0.0862)$). The highest simulated mercury concentration in an age 3 largemouth bass at WCA 3A-15 for the 500 simulation was $1.90 \mu\text{g g}^{-1}$ wet muscle.

It is noteworthy that the distributions for atmospheric Hg(II) deposition and predicted fish mercury concentrations were both lognormal. The extremes were greater for high loads and concentrations than the low values. Furthermore, while the standard deviation in annual Hg(II) deposition was 26.4% of the mean rate, the standard deviation for Hg concentration in age 3 largemouth bass was less, only 5.2% of the mean concentration. This was because there are dampening effects within the marsh which result in mercury concentrations in age three fish not varying as dynamically as the annual atmospheric Hg(II) loadings. Most obviously, age 3 fish integrate their mercury accumulation over a three year period. Second, it takes time for changes in loading to translate into different exposure to the fish because of the steps involved between Hg(II) deposition and mercury concentrations in the diet of fish. The dynamics of the system response to a change in load are examined in the next section.

7.2 How fast does the WCA 3A-15 marsh respond to changes in atmospheric Hg(II) deposition?

Figure 26 shows that WCA 3A-15 is predicted to respond significantly within the first decade following Hg(II) loading reductions. Regardless of the magnitude of the load reduction, fish mercury concentrations are predicted to change by 50% of the ultimate response within 6-7 years (Figure 26). Within 22 years, 90% of the ultimate predicted response has occurred. Figure 31 shows that these predictions are not significantly altered because of uncertainty regarding true current Hg deposition rates and the effects of recalibration to different estimates of current deposition. The actual magnitude of the change in fish Hg is of course dependent on the magnitude of the load reduction, as shown in Figures 23 through 25.

Mercury concentrations in the marsh do continue to change very slightly beyond 100 years after a load reduction. We tested this by comparing the predicted fish mercury concentrations after 100

years with those 1000 years after a load reduction. Total mercury concentrations in water changed by less than 0.5% from 100 to 1000 years, while mercury concentrations in age 5 largemouth bass changed by less than 1.5% during the same period.

7.3 Processes Controlling Hg Concentrations and Dynamics at WCA 3A-15

Hg(II)

Figures 21 and 22 show the predicted long-term average annual fluxes for Hg(II) and methylmercury at WCA 3A-15 respectively. Since concentrations in any given compartment depend on both sources and sinks, it is important to look at both the loading and removal aspects of the mass balances.

Hg(II) in WCA 3A-15 surface waters is very dynamic, due to the shallow waters and relatively rapid kinetics of some processes relative to lake environments. Hg(II) loading was primarily atmospheric in the simulations, but this is affected somewhat by the size and geometry assigned to the marsh cell being modeled. Similar to Fitz *et al.*, (1996) in their modeling of nutrient dynamics in the Everglades, we chose a 1 km x 1 km area as representative of conditions at 3A-15. Segregating the modeled system unit of interest into a set of smaller cells to better represent spatial heterogeneity, a smaller cell size would result in water flowing through the individual cell in a shorter time period than the entire system unit, although the overall hydrologic characteristics of the system unit would not change. When comparing fluxes on an areal basis, this in turn would increase the relative importance of surface inflows as a mercury source *for a given cell*.. The sensitivity analysis (Figure 27) suggested that the surface flowrate and hydraulic residence times were significant but secondary, and suggests that our choice of cell size is probably adequate. Future work funded by FDEP with E-MCM will involve setting up the model as a series of linked cells rather than as a CSTR, thus enabling us to test the effects of cell size more explicitly and rigorously.

Wet and RGM deposition were both important sources of Hg(II) to the marsh (Keeler *et al.*, 2000). We used a leaf area index of 3.0 and backed out the concentrations of atmospheric RGM that would generate the monthly RGM deposition rates provided by Keeler *et al.*, (2000). These monthly atmospheric RGM concentrations ranged from 10.8 to 22.5 pg m⁻³.

In our calibration, most of the macrophyte related Hg(II) loading occurred as throughfall which in turn derived most of its mercury from the atmosphere rather than root uptake. The relative magnitude of throughfall versus litter was influenced by the ability of rain to wash off mercury from macrophyte leaves. This washoff effect is unquantified and should receive future attention.

The predicted total load of mercury to the marsh via combined litter and throughfall was 10.85 µg m⁻² marsh yr⁻¹. Only 15% of this total (1.67 µg m⁻² marsh yr⁻¹) originated from root uptake of Hg(II). These initial results suggest that most of the mercury in litter and throughfall (combined) is derived from the atmosphere and represents a new source of mercury rather than recycling of mercury from roots.

Furthermore, predicted root uptake of porewater Hg(II) on an annual basis (1.8 µg m⁻² marsh yr⁻¹ = 50% macrophyte areal coverage * 3.6 µg m⁻² macrophyte covered area yr⁻¹) was incapable of supplying volatilization rates over macrophytes reported by Lindberg *et al.*, (1999), which were orders of magnitude higher. To achieve higher mercury transpiration rates, we would need one or both of the following: (1) higher predicted porewater concentrations of Hg(II), which ranged from 1.4 to 3.6 ng L⁻¹ in the four sediment layers and were of the same general magnitude as

measurements by Gilmour *et al.*, (1998b), or (2) higher transpiration rates. Our transpiration rates were on the order of 10 g H₂O per g dry biomass per day, equivalent to approximately 1.5 to 2.0 m yr⁻¹.

The primary removal mechanism for Hg(II) at WCA 3A-15 is predicted to be burial (Figure 21), accounting for 63% of total Hg(II) load to the system. Predicted concentrations of Hg(II) in sediments were sensitive to the rate of particle sedimentation. The predicted response dynamics of the marsh were also significantly influenced by burial. Faster sedimentation rates would lead to faster system responses. The particle budget for the marsh is therefore important in terms of loadings, predicted concentrations and predicted response dynamics for Hg(II).

Methylmercury

The dominant predicted source for methylmercury at WCA 3A-15 is in-situ production (6.7 µg m⁻² yr⁻¹), 80% of total MeHg load predicted for the marsh. In our simulations for WCA 3A-15 we calibrated methylation to occur in sediments, and there was no methylation by periphyton, although these are both ongoing topics of investigation. Atmospheric deposition of methylmercury appears to be a minor source – less than 3% of the total methylmercury load to the marsh. The prediction that local production of methylmercury is the major source to WCA 3A-15 is consistent with the hypothesis that local site factors are driving the variability and “hot spots” observed for methylmercury across the Everglades. Several significant loss mechanisms were predicted for methylmercury, including photodegradation, outflow, biological demethylation, and to a lesser extent burial.

The response of methylmercury concentrations in the marsh to changes in Hg(II) loadings depends on the rate at which methylation responds to changes in Hg(II) loading, and the rate at which existing methylmercury concentrations in the system can adjust to changes in methylmercury supplied. We did not resolve within our study which of these two rates controls the response of methylmercury concentrations to changes in Hg(II) loading.

7.4 Effects of Atmospheric Hg Deposition on Fish Mercury Concentrations

Figures 23 and 24 illustrate that in the longer term, fish mercury concentrations are predicted to respond significantly to changes in atmospheric Hg(II) deposition. A linear relationship between atmospheric Hg(II) deposition and fish mercury concentrations is predicted, but the slope is not 1.0, i.e. there is not a 1:1 relationship predicted between atmospheric Hg(II) deposition and mercury concentrations in age 3 largemouth bass. A load reduction of 75.6% is needed for long-term average mercury concentrations in age 3 largemouth bass to drop to 0.5 µg g⁻¹ wet muscle. If we use the age 3 largemouth bass concentration exceeded 5% of the years as a standard (1.81 µg g⁻¹ wet muscle), a decrease in atmospheric Hg(II) deposition of 79% is needed to reduce mercury concentrations from 1.81 to 0.5 µg g⁻¹ wet muscle.

Based on the predicted response curve, fish mercury concentrations would still be 8.23% of current values even without any atmospheric (Hg(II) deposition. This is because there is atmospheric methylmercury deposition in all simulations, and this deposition was not changed in tandem with reductions in Hg(II) deposition. This assumption should be reviewed in any future assessments. Furthermore, there is some remobilization of some methylmercury from deep sediment layers via porewater uptake by macrophytes. Over the course of 100 years, Hg(II) and methylmercury concentrations in these deeper sediments are not significantly affected by changes in atmospheric mercury deposition in the simulations. This added another source of mercury to

the overlying active marsh system; a source which would continue for long periods in the absence of atmospheric Hg(II) deposition.

The predicted long-term response of fish mercury concentrations to changes in atmospheric Hg(II) deposition and concentrations (i.e. linear but with a non-zero intercept), is governed, and to some extent uncertain, as a result of our current understanding of mercury cycling and the resulting assumptions in the model. Specifically, the following assumptions had a significant impact on the shape of the dose-response curve:

- Methylation depends on a bioavailable fraction of porewater Hg(II)
- Porewater Hg(II) concentrations are not currently at saturation. For example it is plausible that additional Hg(II) loading could result in precipitation of the excess Hg(II) as cinnabar, and no change in porewater Hg(II). We do not have cinnabar forming in any of the loading scenarios we examined with our calibration.
- Methylmercury and Hg(II) concentrations in inflows were assumed to be reduced by the same percentage as Hg(II) deposition in scenarios with load reductions. This is to some extent a cyclical assumption, since the assumption regarding inflow concentrations is based to some extent on the model results for the cell being modeled.
- Atmospheric methylmercury loading was held constant, and assumed not to change in proportion to changes in atmospheric Hg(II) deposition. The validity of this assumption is unknown, and depends on the origin of atmospheric methylmercury.

Thus we interpret the predicted response of fish Hg to load reductions in this study to reflect the current level of understanding. This level of understanding is currently inadequate however to place strong confidence in the predictions. The validity of the above assumptions needs resolution.

Furthermore, uncertainty and natural year-to-year variability associated with input values for E-MCM is not reflected in the analysis, with the exception of Hg(II) and MeHg loading rates. This uncertainty would be best accommodated through a Monte Carlo approach. A Monte Carlo version of E-MCM was under development at the time of report preparation.

It is important to recognize that fish mercury concentrations in largemouth bass are sufficiently elevated for some larger fish that it may not be practical or even theoretically possible to bring concentrations below $0.5 \mu\text{g g}^{-1}$ wet muscle on the basis of local anthropogenic Hg(II) load reductions alone. For example, the field measurements of muscle Hg concentrations for larger bass over 35 cm are limited ($n=3$), but exceeded $3 \mu\text{g g}^{-1}$ wet muscle in all cases (Figure 20). Assuming at best a 1:1 response to a change in atmospheric Hg(II) deposition, these fish would need to drop by a factor of six to reach $0.5 \mu\text{g g}^{-1}$. This decrease is roughly equivalent to the estimated increase in mercury loading to the Everglades over pre-industrial loadings derived by Delfino et al. (1994) from sediment cores. Assuming that these inferred increases are from both local and larger scale sources, it is plausible that reductions in Hg(II) loading to WCA 3A-15 may significantly reduce fish mercury concentrations, but still be inadequate to reduce concentrations below $0.5 \mu\text{g g}^{-1}$ wet muscle, even if all anthropogenic contributions to Hg(II) deposition are eliminated.

8. Conclusions

Overall, E-MCM was calibrated to reasonably fit observations for total and methylmercury at WCA 3A-15. The model predicts a linear, but not 1:1 long-term response in fish mercury concentrations to sustained reductions in atmospheric Hg(II) deposition. Mercury concentrations in age 3 largemouth bass are predicted to achieve 50% of the ultimate response within 6 to 7 years and 90% within 20 to 25 years following sustained load reductions. To reach a target of age 3 largemouth bass concentrations not exceeding $0.5 \mu\text{g g}^{-1}$ wet muscle for 95% of the years, a reduction of approximately 79% in atmospheric Hg(II) deposition is needed. Some larger largemouth bass at WCA 3A-15 may stay above $0.5 \mu\text{g g}^{-1}$ wet muscle on a long-term average basis regardless of reductions in Hg(II) emissions.

There are several gaps in the state of knowledge of mercury cycling in aquatic systems which resulted in modeling assumptions and impose uncertainty regarding the predicted magnitude and timing of the relationship between mercury deposition and fish mercury concentrations. These gaps should be addressed in future studies and include the location and governing factors for methylation and demethylation, and fluxes associated with vegetation and particles (litter, throughfall, sedimentation, decomposition). Furthermore, uncertainty and natural year-to-year variability associated with input values for E-MCM should be included in future analyses via a Monte Carlo approach. Finally, the lack of a long-term Hg(II) deposition dataset required us to synthesize a dataset to estimate the effects of year-to year variations in Hg(II) deposition. Longer periods of record will be helpful for any future assessments.

Acknowledgments

We wish to thank the agencies funding this work and the exceptional team researching mercury cycling in the Everglades who provided information essential to our modeling efforts. In particular we thank the funding and support of Tom Atkeson of the Florida Department of Environmental Protection, Larry Fink of the South Florida Water Management District and Ruth Chemerys and Rochelle Araujo of the US EPA. It was our good fortune to work with the ACME research team led by Dave Krabbenhoft (USGS) and including Cynthia Gilmour and Andrew Heyes (Academy of Natural Sciences), Jim Hurley (Wisconsin DNR/University of Wisconsin), Lisa Cleckner and Sue King (University of Wisconsin), Paul Garrison (Wisconsin DNR), Mark Marvin DiPasquale, George Aiken and Mike Reddy (USGS), and Ted Lange (Florida Fish and Wildlife Conservation Commission).

9. References

- Ambrose, R.B. Jr., K.J. Shell and I.Tsiros. 1997. South Florida Mercury Screening Study Part 1 – Mercury in Everglades Marsh. US EPA Office of Research and Development, National Exposure Research Laboratory, Ecosystems Protection Division, Athens, GA. January 1997.
- Cleckner, L.B., P.J. Garrison, J.P. Hurley, M.L. Olson and D.P. Krabbenhoft. 1998. Trophic transfer of methyl mercury in the northern Florida Everglades. *Biogeochemistry* 40(2/3): 347-361.
- Delfino, J.J, T.L. Crisman, J.F. Gottgens, B.E. Rood, and C.D.A. Earle. 1993. Spatial and temporal distribution of mercury in Everglades and Okefenokee wetland sediments. Final Project Report, April 1, 1991 – June 30, 1993. Volume I. Submitted to Florida Department of Environmental Protection, Tallahassee, FL. Department of Environmental Engineering Sciences, University of Florida, Gainesville, FL.
- Delfino, J.J, B.E. Rood, J.M. Andes, and C.D.A. Earle. 1994. Mercury spatial heterogeneity in Everglades soil cores and a comparison of mercury accumulation in wetlands and associated lakes. Final Project Report. Submitted to Florida Department of Environmental Protection, Tallahassee, FL. Department of Environmental Engineering Sciences, University of Florida, Gainesville, FL.
- Fitz, H.C., E.B. DeBellevue, R. Costanza, R. Boumans, T. Maxwell, L. Wainger, and F.H. Sklar. 1996. Development of a general ecosystem model for a range of scales and ecosystems. *Ecol. Modelling* 88: 263-295.
- Gill, G.A., W.M. Landing, and C.D. Pollman. 1999. Florida Atmospheric Mercury Study (FAMS). Data Dictionary, Version 2.0. Submitted by Florida State University, Department of Oceanography to Florida Department of Environmental Protection, Tallahassee, FL and Electric Power Research Institute, Palo Alto, CA.
- Gilmour, C.C., G.S. Riedel, M.C. Ederington, J.T. Bell, J.M. Benoit, G.A. Gill, and M.C. Stordal. 1998a. Methylmercury concentrations and production rates across a trophic gradient in the northern Everglades. *Biogeochemistry* 40(2/3): 327-345.
- Gilmour, C.C., A. Heyes, J. Benoit, G. Riedel and J.T. Bell. 1998b. Distribution and Biogeochemical Control of Mercury Methylation in the Florida Everglades. Data Report March 1995 through July 1997. The Academy of Natural Sciences Estuarine Research Center, MD.
- Guentzel, J.L., W.M. Landing, G.A. Gill, and C.D. Pollman. 1995. Atmospheric deposition of mercury in Florida: The FAMS project (1992-1994). *Water Air Soil Poll.* 80: 393-402.
- Harris, R.C. and R.A. Bodaly. 1998. Temperature, growth and dietary effects on fish mercury dynamics in two Ontario Lakes. *Biogeochemistry* 40: 175-187.
- Hewett and Johnson 1992. Fish Bioenergetics Model 2. Published by the University of Wisconsin Sea Grant Institute (WIS-SG-91-250).

Hurley, J.P., D.P. Krabbenhoft, L.B. Cleckner, M.L. Olson, G.R. Aiken and P.S. Rawlik Jr.. 1998. System controls on the aqueous distribution of mercury in the northern Florida Everglades. *Biogeochemistry* 40(2/3): 293-310.

HydroQual, Inc. 1997. SFWMD Wetlands Model: Calibration of the Coupled Periphyton/Vegetation Model to WCA-2A. October 21, 1997

Keeler, G.J., F. J. Marsik, K.I. Al-Wali and J. T. Dvonch. 2000. Project Final Technical Report - Modeled Deposition of Speciated Mercury to the SFWMD Water Conservation Area 3A: 22 June 1995 to 21 June 1996. Project Description and Results. The University Of Michigan Air Quality Laboratory. Ann Arbor, Michigan 48109

Krabbenhoft D.P., J.P Hurley, ML. Olson & L.B. Cleckner. 1998. Diel variability of mercury phase and species distributions in the Florida Everglades. *Biogeochemistry* 40: 311-325.

Limno – Tech 1996

Lindberg, S.E., H Zhang and T.P. Meyers. 1998. Application of Field Methods and Models to Quantify Mercury Emissions from Wetlands at the Everglades Nutrient Removal Project. Final Report. Submitted to L.E. Fink, South Florida Water Management District, West Palm Beach, Florida.

Tetra Tech Inc. 1999a. Dynamic Mercury Cycling Model for Windows 95/NT. A Model for Mercury Cycling in lakes – D-MCM Version 1.0 – User's Guide and Technical Reference. Prepared for EPRI. April 1999.

Tetra Tech Inc. 1999b. Everglades Mercury Cycling Model for Windows 95/NT. A Model for Mercury Cycling in Everglades Marsh Areas – Draft User's Guide and Technical Reference. Version 1.0 Beta. Prepared for the United States Environmental Protection Agency. June 1999

US EPA. 1999. WWW address: <http://www.epa.gov/OWOW/tmdl/wrkpln2.html>. August 14, 1999.

Winter, T.C. 1981. Uncertainties in estimating the water balance of lakes. *Water Resour. Bull.* 17: 82-115.